Title

Collision Analysis Of Vehicle Following Operations By Two-dimensional Simulation Model: Part I - Effects Of Operational Variables

Permalink

https://escholarship.org/uc/item/28s0m2jq

Author

Chan, Ching-Yao

Publication Date

1997

Collision Analysis of Vehicle Following Operations by Two-Dimensional Simulation Model: Part I – Effects of Operational Variables

Ching-Yao Chan

The contents of this report reflect the views of the authors who are responsible for the facts and the accuracy of the data presented herein. The contents do not necessarily reflect the official views or policies of the State of California. This report does not constitute a standard, specification, or regulation.

CALIFORNIA PARTNERS FOR ADVANCED TRANSIT AND HIGHWAYS

Collision Analysis of Vehicle Following Operations
by Two-Dimensional Simulation Model

I
Effects of Operational Variables

Ching-Yao Chan
California PATH, Headquarters
University of California, Berkeley
Richmond Field Station, Bldg. 452, 1357 S. 46th Street, Richmond, CA 94804-4698, USA
Phone: 510-231-5663, Fax: 510-231-5600, E-mail: cychan@uclink2.berkeley.edu

EXECUTIVE SUMMARY

In operations of intelligent vehicle and highway systems (IVHS), automated vehicles maintain a desired speed and safe distance from the preceding vehicles. The vehicles also maintain their positions within a lane or on their designated path. Since vehicles are equipped with automated control systems to maintain the speed and spacing safely, they are likely to follow each other closely. One of the safety concerns for such systems is the consequences in failure or malfunctioning events when collisions occur. This research project investigates the behaviors of vehicles in collisions, especially when they are closely spaced.

This study uses a two-dimensional simulation program, EDSMAC, which allows longitudinal and lateral movements as well as the yaw motion of vehicles. The simulation model calculates impact forces in collisions and estimates the resulting vehicle damage. The study is an extension of several previous studies at PATH on this subject, which have emphasized on the one-dimensional dynamics of vehicle impacts. The addition of vehicle motions in other axes provides a meaningful representation of real-world crashes.

Collision situations, representing failure or malfunctioning events, are simulated. The subsequent post-impact vehicle trajectories are then analyzed. By varying parameters in simulation cases, one can evaluate the potential effects of such variables in vehicle-following operations.

Through a systematic approach, correlation between the collision consequences and the operating variables in AHS can be established. The results of this analysis may also provide valuable inputs to the design of control systems. Proper emergency handling strategies and control laws may be developed to mitigate collision consequences. These studies are essential in the understanding and improvement of safety design in AHS.

BACKGROUND

In order to evaluate the safety benefits of intelligent vehicle and highway systems (IVHS) or automated highway systems (AHS), it is essential to understand the behavior of automated vehicles when failures or malfunctions occur. Studies on vehicle damage, post-impact vehicle movements, and occupant injuries when collisions occur help evaluate the safety hazards in failure events. They provide insight for identifying the criteria of safety design in vehicle following operations.

Previous studies by Hitchcock (1) investigated vehicle collisions in several types of potential AHS operations. In his analysis, Hitchcock used an inelastic collision model in which vehicles would remain in contact and become a v-mass after an impact. A series of studies was conducted by Tongue and his students (2,3,4) on the collision dynamics of vehicle platoons. They utilized a reduced-order vehicle model to examine the dynamics of a platoon in emergency maneuvers. These studies deal with collisions in the longitudinal direction only.

In real-world accidents, vehicle crashes result in a variety of post-impact behaviors. In some cases, some vehicles may remain in contact for a considerable long period of time. In other cases, vehicles separate from each other after the initial impact and continue their motions in separate trajectories and may become involved in further impacts with other objects.

In related work, the author adopted a different model and examined the effects of certain critical variables in vehicle following. (5, 6) The work extended the collision analysis by Hitchcock and Tongue by applying a two-dimensional simulation model to evaluate the consequences of vehicle collisions in malfunctioning or failure events.

SIMULATION MODEL

The analysis of vehicle collisions in this work is conducted with a simulation program developed by Engineering Dynamics Corporation (EDC). The software package, EDSMAC (Engineering Dynamics Corporation Simulation Model of Automobile Collisions), is used for the analysis of a single or two-vehicle accident. It is based on a program called SMAC (7-9) initially developed and validated by Calspan Corporation and subsequently improved by EDC (10-13). EDSMAC uses a set of assumed or estimated initial conditions, including positions and velocities, and predicts the outcome of a collision. Engineers and accident reconstructionists have been using this simulation program to analyze vehicle dynamics and the damage resulting from crashes. Researchers have found that the program yields reasonable results with sound input data (14-19).

In its vehicle model, EDSMAC allows the longitudinal and lateral movements as well as the rotational motion about the vertical axis of vehicles on a horizontal plane. If a contact between vehicles is detected, the collision phase is analyzed. The external forces can be applied either at the tire/road interface or between the vehicles. The vehicle exterior is assumed to have homogeneous stiffness.

In the simulation model, a force proportional to the amount of crush is exerted as the body of a vehicle is crushed. This is accomplished by dividing the vehicle's perimeter into equally spaced intervals. Each of these intervals forms a pie-shaped wedge having its focus at the center of gravity of the vehicle. By knowing where the vehicles are with respect to each other, EDSMAC locates the wedges which are in contact and equalize the force between them. The resulting summation of forces dictates the motion of each vehicle due to the collision. This process continues for each collision time increment until the vehicles are no longer in contact. Default values of the crush stiffness data according to vehicle class category are used in the simulation. (13)

EDSMAC allows the direct entry of vehicle data by users or the selection of default values. The vehicles are categorized by their wheelbase into several classes. Class I and II are small passenger cars while Classes III to V are medium to large cars. In this paper, default values of vehicle parameters provided by EDSMAC are used in the simulation. (13)

Appendix A contains exemplar pages of the program EDSMAC and tables showing the default values of different vehicle classes.

SIMULATION SCENARIOS AND ASSUMPTIONS

In real-world accidents, vehicle crashes result in a wide range of post-impact behaviors. The post-impact motions of vehicles involved in a collision are affected by the following factors:
1. collision conditions, such as vehicle orientation and types of impacts;
2. vehicle parameters, such as size, weight and structural strength;
3. vehicle states, such as translational and rotational speed and acceleration;
4. vehicle control input, such as throttle, braking, and steering;
5. roadway states, such as surface friction, curvature, grade, and roadside hazards.
6. Tire-roadway interactions, such as friction coefficient and tire traction forces.

Some of the variables in the list above are varied in this study to investigate their effects, such as vehicle sizes and collision conditions. Some variables are not altered due to the limitations of the simulation program, such as roadway grade or elevation. Others, such as steering or braking inputs, will be examined in the next phase of study and presented in a following research report.

The simulation in this paper is conducted for a two-vehicle impact scenario described as follows:
1. The two vehicles are proceeding straight and no steering inputs are entered before, during, or after the impact.
2. The leading vehicle at time zero began braking with a constant 0.7 g deceleration and the following vehicle applied no acceleration or deceleration. Throughout the simulation duration, the braking of the leading vehicle remains applied.
3. No other objects or vehicles come into contact with the two vehicles in question.

The simulation scenario is chosen to reflect one of the most critical failure conditions that may occur. Such scenarios may result from the following malfunctions or failures:
1. a miscommunication from the leading vehicle to the following vehicle, and a failure in the range sensor on the following vehicle, or
2. a failure in brake actuation on the second vehicle.

Due to the limitations of the simulation models, the problem is formulated to analyze two-vehicle collisions only. The existing software does not allow a third vehicle or object to be involved in the collision process. The motions of the vehicles are restricted on a horizontal plane.

In scenarios with different initial spacing between the two vehicles, the first collision starts at different time instants after the initial application of braking in the leading vehicle. For comparison of results in different cases, the simulation is run for the same time period after the initial impact. In the cases presented in the next section, the simulation is terminated after four seconds of vehicle motions from the initial impact. A duration of four seconds is chosen based on the following reasoning:
1. A deviation in vehicle states or roadway geometry in real-world situations may render the simulation unrealistic and inapplicable. Such deviations may result from a change of tire angles, impacts with other objects, roadway curvature and elevation, or vehicle control being activated, etc.
2. In simulation cases with both vehicles starting at 105 kmph (65 mph) and initial spacing of 1-10 m, the two vehicles will have traveled about 90-105 m at the termination of simulation. The vehicle motions are likely to be affected by factors described in (1) after such distances.
3. In most cases the delta-V of impacts gradually diminishes as time goes on. The simulation in the initial few seconds provide more critical information than in later periods.

In order to evaluate the criticality of operational variables, certain parameters in the simulated scenarios are varied in different sets of cases. The variables include:
1. spacing between the two vehicles at the beginning of the simulation,
2. lateral offset of vehicle centerlines at initial impact,
3. classes of vehicles, and
4. vehicle speed.

Descriptions of these simulation scenarios and results are given in the next section.

SIMULATION RESULTS

In the assessment of vehicle collisions, the following consequences of collisions are of particular interests in our studies:

1. Equivalent Delta-V: This is the speed differential between two vehicles at the time of impact and is often a good indicator of the potential occupant injuries.
2. Vehicle Damage: This is the physical destruction to the vehicle bodies and thus a direct measure of property and potential functionality loss.
3. Lateral Deviation: This is the lateral movement of a vehicles from its original path. In the simulated cases, it is measured by the maximum lateral position of the center of gravity (CG) of a vehicle in either direction.
4. Vehicle Rotation: This is the yaw angle of a vehicle. The maximum yaw angle of each vehicle in either the clockwise or the counter-clockwise direction is used for comparison.
5. Lane Departure Time: This is the elapsed time from the initial collision to the instant when a vehicle CG leaves its original lane. In this paper, the lane departure time is defined as the time when the lateral movement of a vehicle CG exceeds 0.9 m.
6. Speed and Yaw Angle at Lane Departure Time: These variables represent the potential hazards incurred by the departing vehicle.

The first two measures are directly linked to the evaluation of vehicle structure and occupant injuries, which requires further analysis and a wide scope of studies. The last measure is not included in the discussions here because the simulation does not allow impacts with other objects. We will focus on measures 3-5 in the following discussions.

In the first set of simulation cases, the two vehicles start at 105 kmph (65 mph) with a selected initial spacing and a given lateral offset. The lateral offset is defined as the distance between the longitudinal axes of the two vehicles. The leading vehicle is assumed to be in the center of a lane while the following vehicle is offset to the left side of the centerline. The simulation is repeated for lateral offsets of 0.15, 0.30, 0.45, 0.60, and 0.75 m. The initial spacing is then changed to another value before the iterations for different lateral offsets repeat. The initial spacing used in the simulations includes values of 1, 3, 5, and 10 m. The sizes of the two vehicles are also chosen to vary with the following three formations:
1. Class III vehicle leading and Class III following (Formation I),
2. Class I leading and Class IV following (Formation II),
3. Class IV leading and Class I following (Formation III).
Here the classes of vehicles are defined in EDSMAC with default values for their sizes, inertia, and crush characteristics.

The results of the first set of simulations are shown in Figures 1-28. Figures 1 and 2 depicts the variation of lateral deviations of the leading and the following vehicles in Formation I with various initial spacing and lateral offset. Figures 3 and 4 are the corresponding results for Formation II while Figures 5 and 6 are those of Formation III. The results are represented differently in Figures 7-14, where the initial spacing is fixed in each figure with different formations. Figures 15-28 show the lane departure time corresponding to each set of data given in Figures 1-14.

The observations from the first set of simulation cases can be summarized as follows:
1. For a given speed and an initial spacing, the lateral deviations of both the leading and the following vehicles become greater as the lateral offset increases. This is illustrated in Figure 1, 3, and 5.
2. The pattern described in (1) holds true for the several values of initial spacing
3. The pattern described in (1) is valid for all three different formations.
4. The lateral deviations do not increase linearly, but fluctuates, with larger lateral offset and larger initial spacing.
5. The lateral deviations in formation II are the greatest and those in formation III are smallest.
6. In general, the lane departure time is shorter for larger lateral offsets and larger initial spacing.
7. The lane departure time for most cases are between 1 to 3 seconds but it falls to 0.7 seconds for extreme cases.
8. In accordance with (5), the lane departure time is shortest for formation II and longest for formation III.
9. In certain cases, the following vehicle leaves the original lane from the left side shortly after the initial collision because it starts with a position left to the centerline.
10. In a majority of cases, the leading and the following vehicles both proceed further off the lane to the right as they move forward after the initial collision. In a smaller number of cases, they rotate and move back toward the center of the lane, creating a wavy trajectory. In a few rare cases, the yawing motions are such that the leading vehicle rotates out of the way of the following vehicle and the two vehicles become separated.
11. Some cases, as explained in (10), do not record lane departure time when the simulations are terminated.

In the second set of cases, both vehicles start at a speed of 105 kmph and a lateral offset of 0.30 m. The simulation is repeated for various initial spacing from 1 to 10 m with an increment of 1m. The results are shown in Figures 29-34. In Figures 29-32, the lateral deviations and yaw angles of the leading and the following vehicles are plotted

for three different formations with the initial spacing changing from 1 to 10 m. Figures 33 and 34 illustrate the trends of the lane departure time for the leading and the following vehicles respectively.

This set of simulations reveals the following patterns:
1. The lateral deviation of the leading vehicle does not increase consistently with the increase in initial spacing. Instead, it fluctuates between 0.4 and 2.8 m with initial spacing of 1 to 10 m for each of the three formations. This is illustrated in Figure 29.
2. The lateral deviation of the following vehicle increases drastically for initial spacing of 5 m or greater for formation II and III, as shown in Figure 30.
3. The yaw angle of the leading vehicle is significantly greater for formation II in cases with initial spacing of 5 m and higher. The vehicle rotates as much as 270 degrees in the counter-clockwise direction. This is depicted in Figure 31.
4. The yaw angle of the following vehicle is relatively small, mostly below 10 degrees, in all three formations, as shown Figure 32.
5. The lane departure time of both vehicles becomes shorter for cases with greater initial spacing.
6. The lane departure time of the leading vehicle is shortest for formation II and longest for formation III.

The third set of cases is simulated with the vehicles starting at 153 kmph (95 mph) and a lateral offset of 0.3 m. Results are given in figures 35-40. In figures 35-36, the lateral deviations and yaw angles of the leading and the following vehicles are plotted for three different formations with the initial spacing changing from 1 to 10 m. Figures 39 and 40 illustrate the lane departure time for the leading and the following vehicles respectively.

The following observations are made from this set of simulations:
1. The lateral deviation of the leading vehicle does not increase consistently with the increase in initial spacing. Instead, it fluctuates between 0.3 and 3.5 m for each of three formations, as shown Figure 35.
2. The lateral deviation of the following vehicle increases drastically for initial spacing of 4 m or greater for formation II and III. This is depicted by Figure 36.
3. The yaw angle of the leading vehicle is significantly greater for formation II in cases with initial spacing of 5 m and higher. The vehicle rotates more than 270 degrees in the counter-clockwise direction, as shown in Figure 37.
4. The yaw angle of the following vehicle is relatively small, mostly below 10 degrees, in all three formations, as shown in Figure 38.
5. The lane departure time of the leading vehicle gradually decreases for cases with larger initial spacing, as shown in Figure 39.
6. The lane departure time of the following vehicle becomes significantly shorter for cases with initial spacing of 5 m or greater, as shown in Figure 40.

To validate the simulation results of the two previous sets, a third set of data is obtained by changing the initial speed to 129 kmph (80 mph). The results are given in Figures 41-46. They correspond to the figures of the two previous cases with similar titles and representations.

A comparison among the results of the cases with initial speeds of 105, 129, and 153 kmph, in which the only difference is the starting speed, indicate that the patterns of observed measures are strikingly similar. Both cases show that the lateral deviation of the leading vehicle is somehow bounded but that of the following vehicle becomes much greater for large initial spacing. On the other hand, the yaw angle of the leading vehicle increases drastically for cases with large initial spacing while that of the following vehicle is limited. In many of these cases, the leading vehicle rotates away from the following vehicle and comes to a stop while the following vehicle proceeds forward in a separate trajectory.

SUMMARY

The study of vehicle collisions is important for evaluating the potential hazards of failure events. This study uses a two-dimensional simulation model to investigate collisions in vehicle following operations. The simulations provide a means for evaluating the effects of operating variables on post-impact vehicle motions.

It can be concluded from the simulations described in this paper that small spacing and small lateral offset in vehicle following offer potential benefits in minimizing post-impact deviations from the original paths and rotation

from the original orientation. The time it takes for a vehicle to depart from its original lane is shorter for those cases with greater lateral deviations and vehicle rotations. Besides the effects of lateral offset, greater delta-V also contributes to greater post-impact motions and shorter lane departure time. The effect of greater delta-V is exemplified in a comparison of cases with different operating speeds.

This study evaluates the consequences of collisions beyond the one-dimensional analysis suggested in previous studies. It provides additional information to help understand post-impact vehicle dynamics. With inputs from studies of this type, the evaluation of safety issues in AHS may be pursued by using a simpler one-dimensional model for macroscopic assessment and more complex simulations for detailed representation of specific conditions.

REFERENCES

1. A. Hitchcock, "Intelligent Vehicle Highway System Safety: Multiple Collisions in Automated Highway Systems," PATH Research Report, UCB-ITS-PRR-95-10.
2. B.H. Tongue, Y-T Yang, M.T. White, "Platoon Collision Dynamics and Emergency Maneuvering I: Reduced Order Modeling of a Platoon for Dynamical Analysis," PATH Research Paper, UCB-ITS-PRR-91-15.
3. B.H. Tongue, Y-T Yang, "Platoon Collision Dynamics and Emergency Maneuvering II: Platoon Simulations for Small Disturbances," PATH Research Paper, UCB-ITS-PRR-94-4.
4. B.H. Tongue, Y-T Yang, "Platoon Collision Dynamics and Emergency Maneuvering III: Collision Models and Simulations," PATH Research Paper, UCB-ITS-PRR-94-2.
5. C. Chan, "Studies of Collisions in Vehicle Following Operations by Two-Dimensional Impact Simulations," ITS American, Sixth Annual Meeting, Houston, Texas, April 1996.
6. C. Chan, "Collision Analysis of Vehicle-Following Operations in AHS," Third World Congress on Intelligent Transport Systems, Orlando, Florida, October 1996.
7. McHenry, R.R., "Development of a Computer Program to Aid the Investigation of Highway Accidents," Calspan Report No. VJ-2979-V-1, DOT HS 800 821, December 1971.
8. Solomon, P.L., "The Simulation Model of Automobile Collisions (SMAC) Operator's Manual," US DOT, NHTSA, Accident Investigation Division, 1974.
9. Noga, T., Oppenheim, T., "CRASH3 User's Guide and Technical Manual," U.S. DOT, January, 1981.
10. T.D. Day, R.L. Hargens, "Differences between EDCRASH and CRASH3," SAE Paper No. 850253.
11. Day, T., Hargens, R., "An Overview of the Way EDSMAC Computes Delta-V," SAE Paper No. 880069, Society of Automotive Engineers, 1988.
12. Engineering Dynamics Corporation, EDCRASH, "Reconstruction of Accident Speeds on the Highway," Version 4.5, June 1989.
13. Engineering Dynamics Corporation, EDSMAC, "Simulation Model of Automobile Collisions," Version 2.4, May 1989.
14. Jones, I.S., "Results of Selected Applications to Actual Highway Accidents of the SMAC Reconstruction Program, " SAE Paper No. 741179, 1974.
15. Jones, I.S., "The Application of the SMAC Accident Reconstruction Program to Actual Highway Accidents," Proceedings of the Eighteenth Conference of the American Association of Automotive Medicine, 1974.
16. R.S. Smith, J.T. Noga, "Accuracy and Sensitivity of CRASH," National Center for Statistics and Analysis, NHTSA, January 1982.
17. A.K. Prasad, "CRASH3 Damage Algorithm Reformulation for Front and Rear Collisions," SAE Paper No. 900098.
18. "Collision Deformation Classification," SAE Technical Report J224 MAR80, March 1980.
19. Day, T., Hargens, R., "Application and Misapplication of Computer Programs for Accident Reconstructions," SAE Paper No. 890738, 1989.

APPENDIX A

The following figures are pages from the user's manual of EDSMAC. (13)

No. Title of Figures
1. A typical screen display of an EDSMAC simulation.
2. A post-simulation display of vehicle damage.
3. A graphic illustration of selected variables of an EDSMAC simulation.
4. The classification of vehicle sizes by their wheel base and the default values of vehicle parameters.
5. Different classes of vehicle stiffness and exemplar vehicles.

Trajectory Simulation

Damage Profiles

Vehicle No. 1 (Rabbit)

Vehicle No. 2 (Chevelle)

EDSMAC Collision Simulation Program

EDSMAC
Damage Profiles

Damage Range No. 1
of 1 Range(s).

CDC ─────────────>
    Veh #1 12FDEW3
    Veh #2 02RPEW4

PSIM (deg) ──────>
    Veh #1   3.0
    Veh #2   98.6

Delta-V (mph) ──>
    Veh #1   42.3
    Veh #2   20.9
    Press ESCape
      to Exit
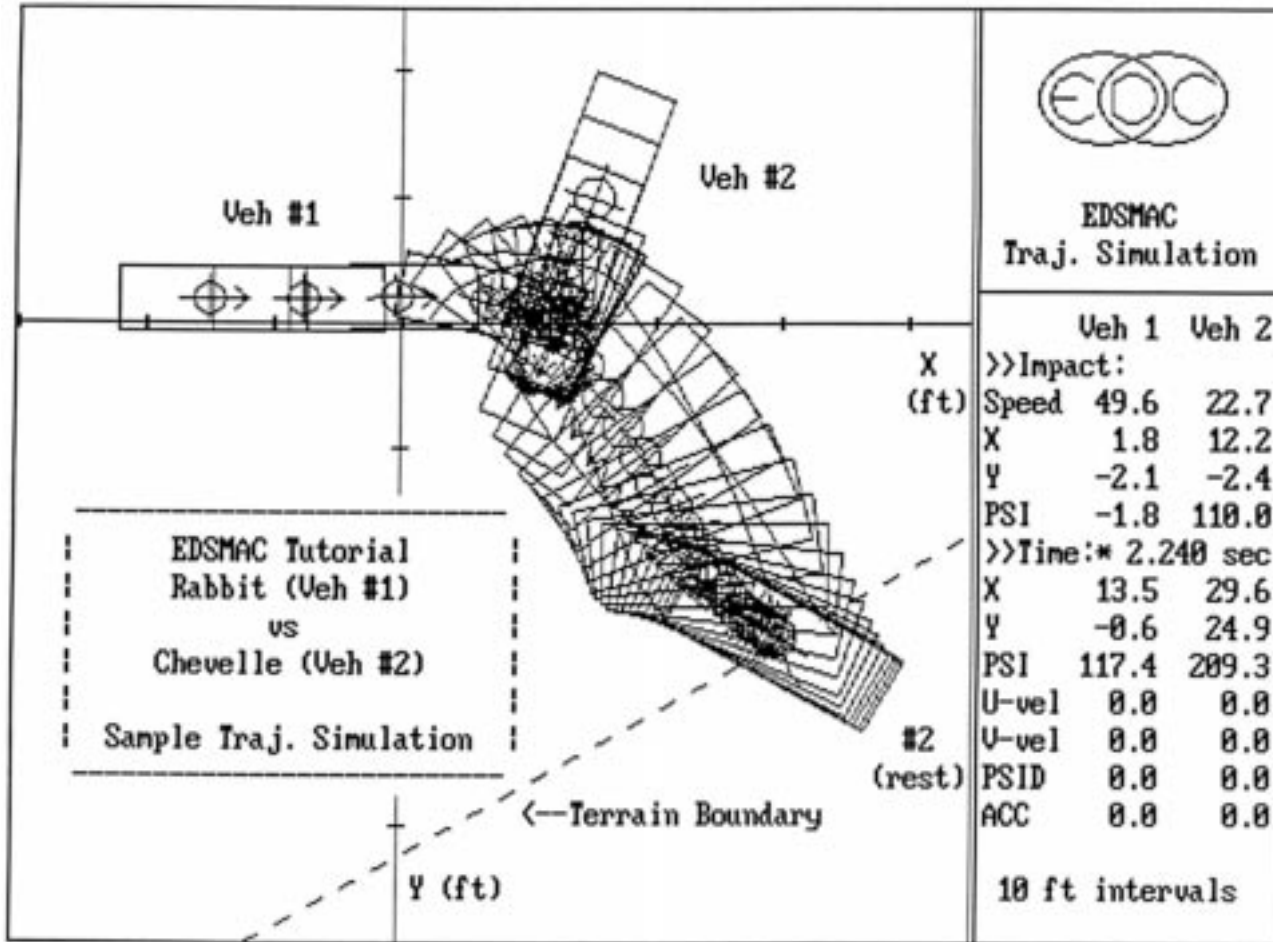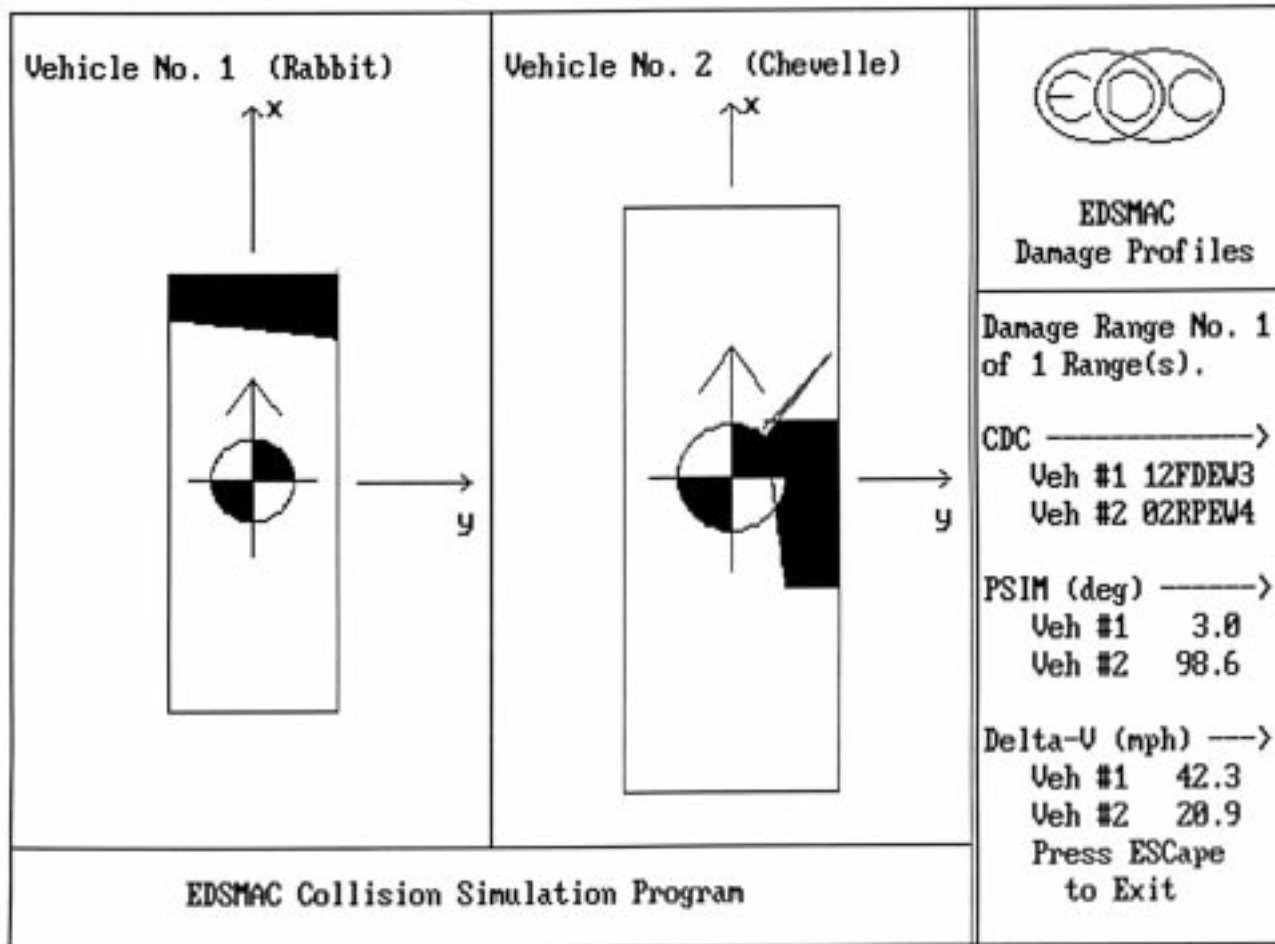
Data Graph
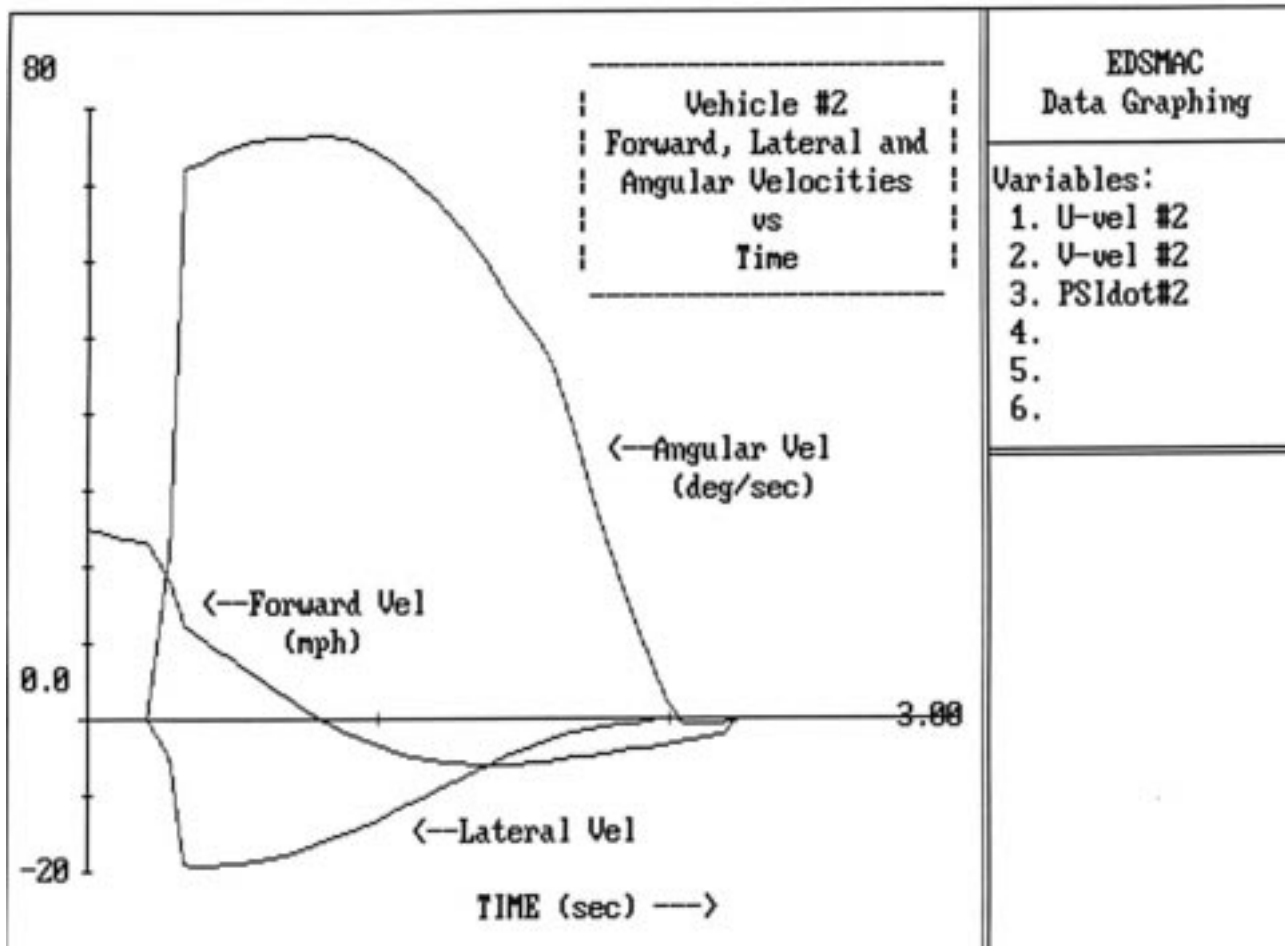
Vehicle Class Categories

PARAMETER	CLASS CATEGORIES								
	1	2	3	4	5	6	7 (VANS)	8/9	10/11
Wheelbase (in)	80.9-94.8	94.8-101.6	101.6-110.4	110.4-117.5	117.5-123.2	123.2-150	109-130	No Data for Category 8 (Pickups) or 9 (Front wheel drive) Select Category 1 - 6 According to Wheelbase	No Data for Category 9 or 10 Barriers not allowed
Track (in)	51.1	54.6	58.9	61.8	63.7	63.7	67.6		
Length (in)	159.8	174.9	196.2	212.8	223.7	229.4	183.6		
Width (in)	60.8	67.2	72.6	77.0	79.8	79.8	79.0		
A (in)	45.1	46.3	51.3	54.7	58.1	60.1	48.5		
B (in)	48.1	50.1	55.5	59.2	63.0	65.1	68.5		
X_f (in)	76.0	83.3	89.8	98.8	101.8	104.2	75.6		
X_r (in)	83.8	91.6	106.4	114.0	121.9	125.2	107.0		
Rsq (in^2)	2006	2951	3324	3741	4040	4229	3713		
I_{zz} (lb-sec^2-in)	11434	23313	30514	41114	50864	58106	41586		
Weight (lb)*	2202	3053	3547	4247	4865	5309	4300		
$C_{alfa,f}$ (lb/deg)	94	131	152	182	209	228	209		
$C_{alfa,r}$ (lb/deg)	88	121	141	168	193	210	193		

LEGEND:
A = Distance from CG to front axle
B = Distance from CG to rear axle
X_f = Distance from CG to front of vehicle
X_r = Distance from CG to rear of vehicle

Rsq = Radius of gyration squared
I_{zz} = Yaw moment of inertia
C_{alfa} = Tire cornering stiffness
* Weight includes 300 lb occupant loading

Vehicle Crush Stiffness Categories

	CLASS CATEGORIES →									
	1	**2**	**3**	**4**	**5/6**	**7**	**8**	**9**	**10/11**
Vehicle Models[**]	Pinto (FRONT) Accord Honda CVCC Prelude Corolla Chevette Fiesta Bobcat Datsun 210 Datsun 310 Arrow Champ Colt Porche 924 Mazda GLC Fiat 124 Spyder Fiat X/19 Datsun 260 ZX Opel MG Miget Tri. Spitfire VW Rabbit VW Scirocco	Pinto (REAR) Chev. Monza Celica ST Celica GT Corona Spirit Pacer Gremlin VW Dasher Vega Skyhawk Omni Sunbird Starfire Mustang (74-) Horizon Fiat 128 Sedan Capri 260 ZX 2+2 Challenger BMW 320i Audi Fox Mazda Cosmo Mazda RX-7 Renault LeCar Saab 900 Saab 99 Subaru	Celica Supra Mustang (-73) AMC Concord Malibu (78-) Monarch Zephyr Fairmont Granada Firebird Cressida Datsun 810 Monte Carlo (78-) Gran Prix (78-) Cutlass (78-) LeMans (78-) Regal Aspen Peugot 604L BMW 528i Volvo (all) Audi 5000	Chevelle (-75) Monte Carlo (-77) Gran Prix (-77) Cutlass (-77) LeMans (-77) Phoenix Chev V-8 (77-) LeSabre (77-) Volare Monaco (77-) Magnum Century LeBaron Riviera (77-) Marquis (77-) LTD (77-) Cordoba Nova Eldorado (79-) Delta 88 (77-) Diplomat T-bird (77-) Seville Ventura Cougar	LeSabre (-76) Chev V-8 (-75) Monaco (-76) Riviera (-76) Marquis (-76) LTD (-76) Eldorado (-76) Delta 88 (-76) T-bird (-76) Olds 98 St. Regis Newport Brghm, DeVille Electra Fleetwood Continental Checker Cab	**VANS** Ford Econo E150 Dodge B-200 Chev G-20 Ford P-500 GMC G-35 GMC G-1500 VW Vanagon **OTHER** Datsun P/U Honcho 4X4 P/U Wagoneer Scout II Chev Blazer	**PICKUPS** Courier El Camino Ford F150 Chev Luv Ford F250 Dodge D-100 Ranchero F10 Ford F100 GMC 1500 Toyota SR5 lg. bed	**FRONT DRIVE** Citation Phoenix Skylark Omega Reliant Aries Escort Lynx	**BARRIERS**
AKV Stiffness (lb/in^2)	59	59	70	51	56	56	56	50	***

[*] For test modes or vehicle models not listed, use a structurally similar category or choose a category by wheelbase dimensions (see Table 3). NASS teams should consult their zone center if in doubt as to proper stiffness category.

[**] Includes all model years unless otherwise specified.

[***] Barriers not allowed. However, barrier simulations can be approximated by choosing a value in the range of 10^3.

LIST OF FIGURES

Figure 1. Maximum Lateral Position of Leading Vehicle with Class III Leading and Class III Following for Various Spacing and Lateral Offset
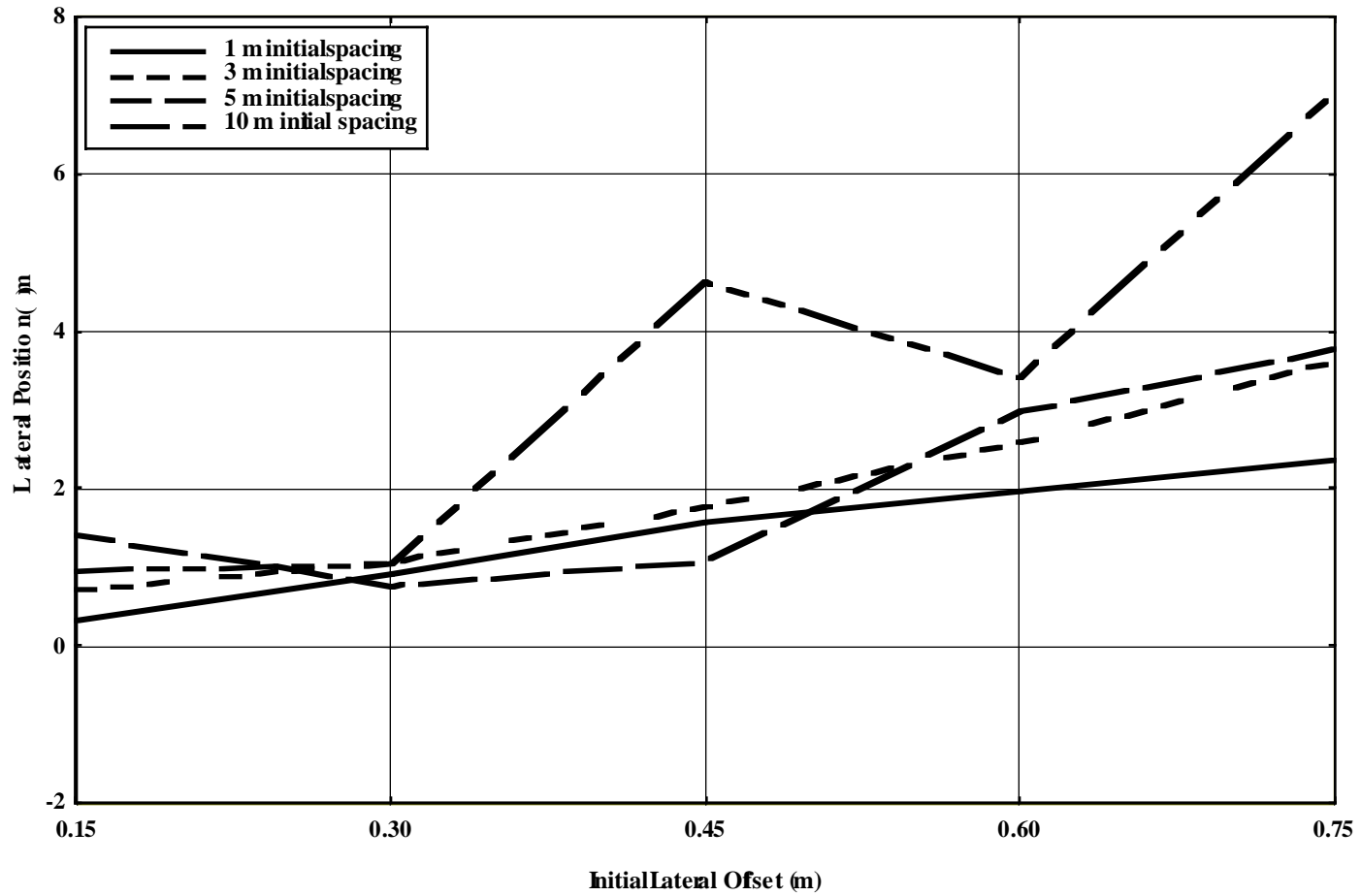
Figure 2. Maximum Lateral Position of Following Vehicle with Class III Leading and Class III Following for Various Spacing and Lateral Offset
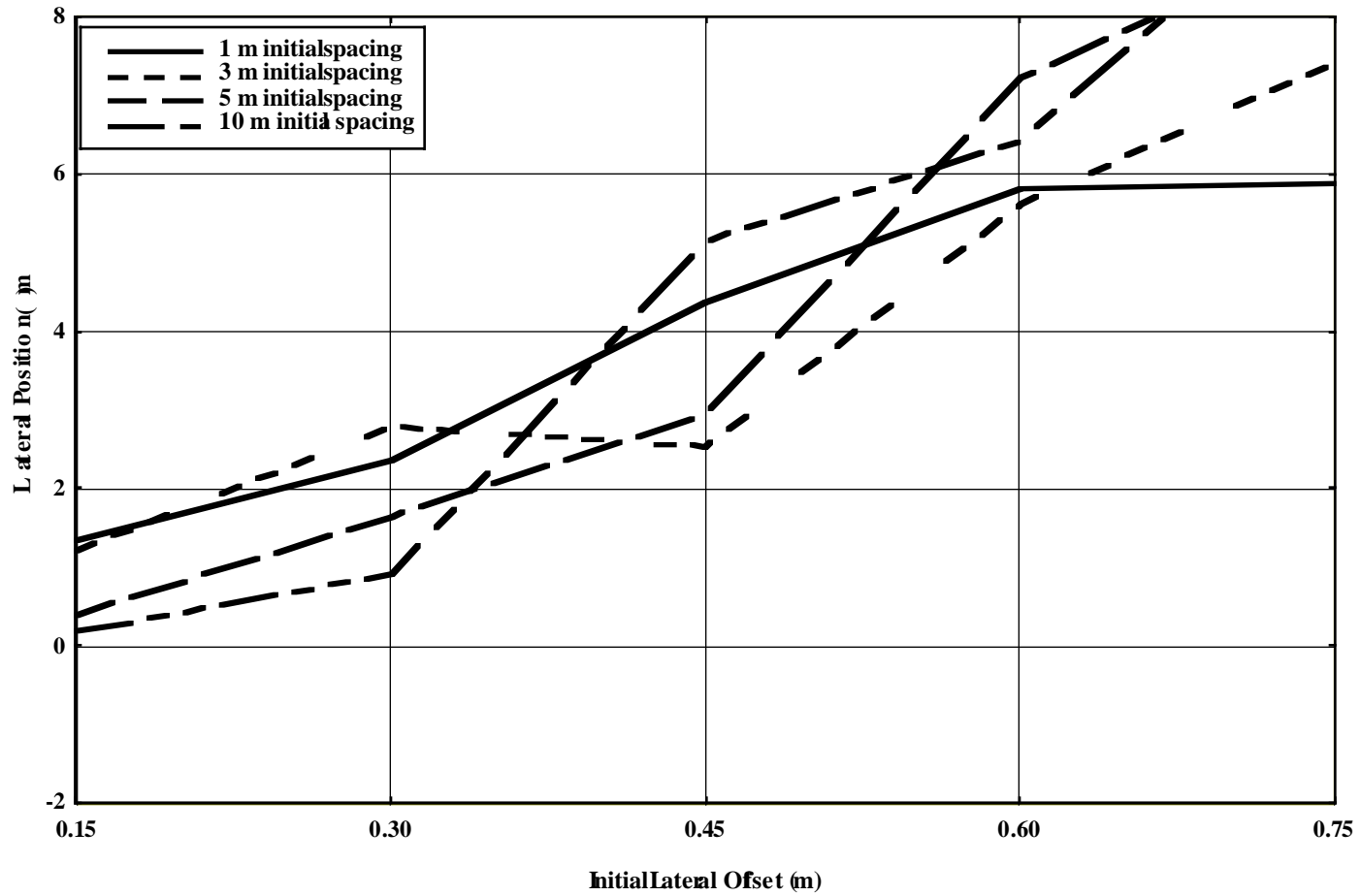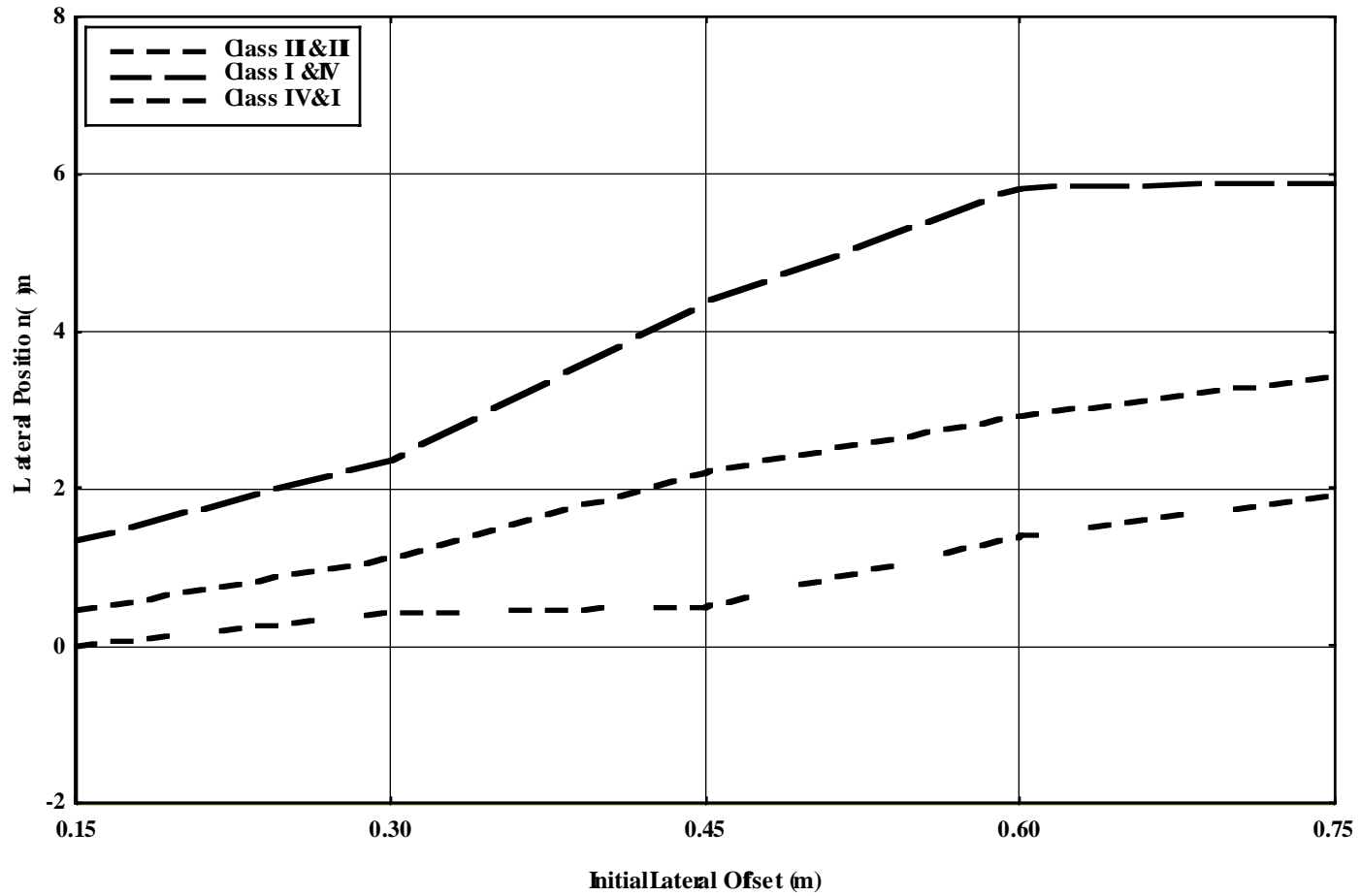
Figure 3. Maximum Lateral Position of Leading Vehicle with Class I Leading and Class IV Following for Various Spacing and Lateral Offset
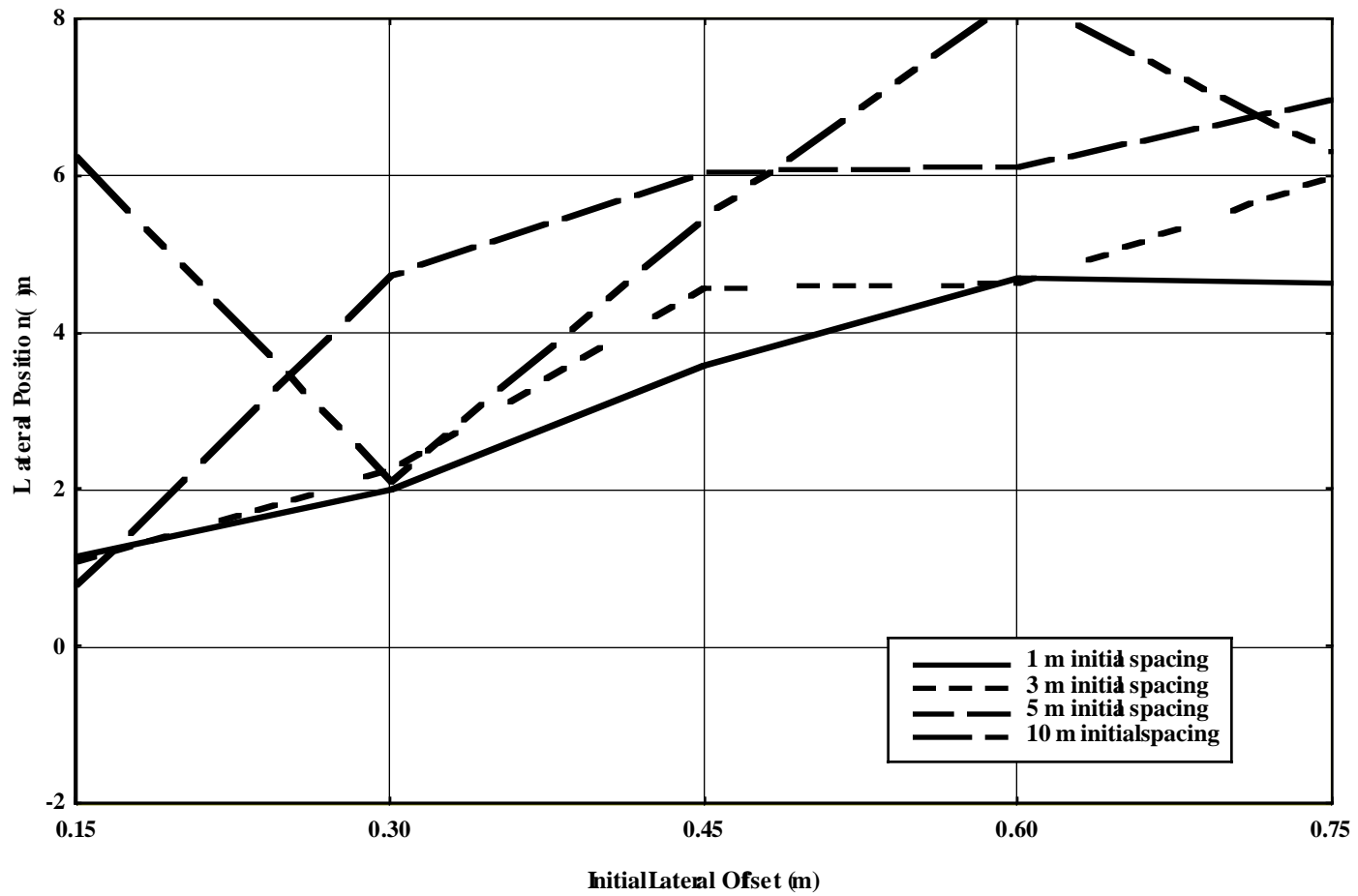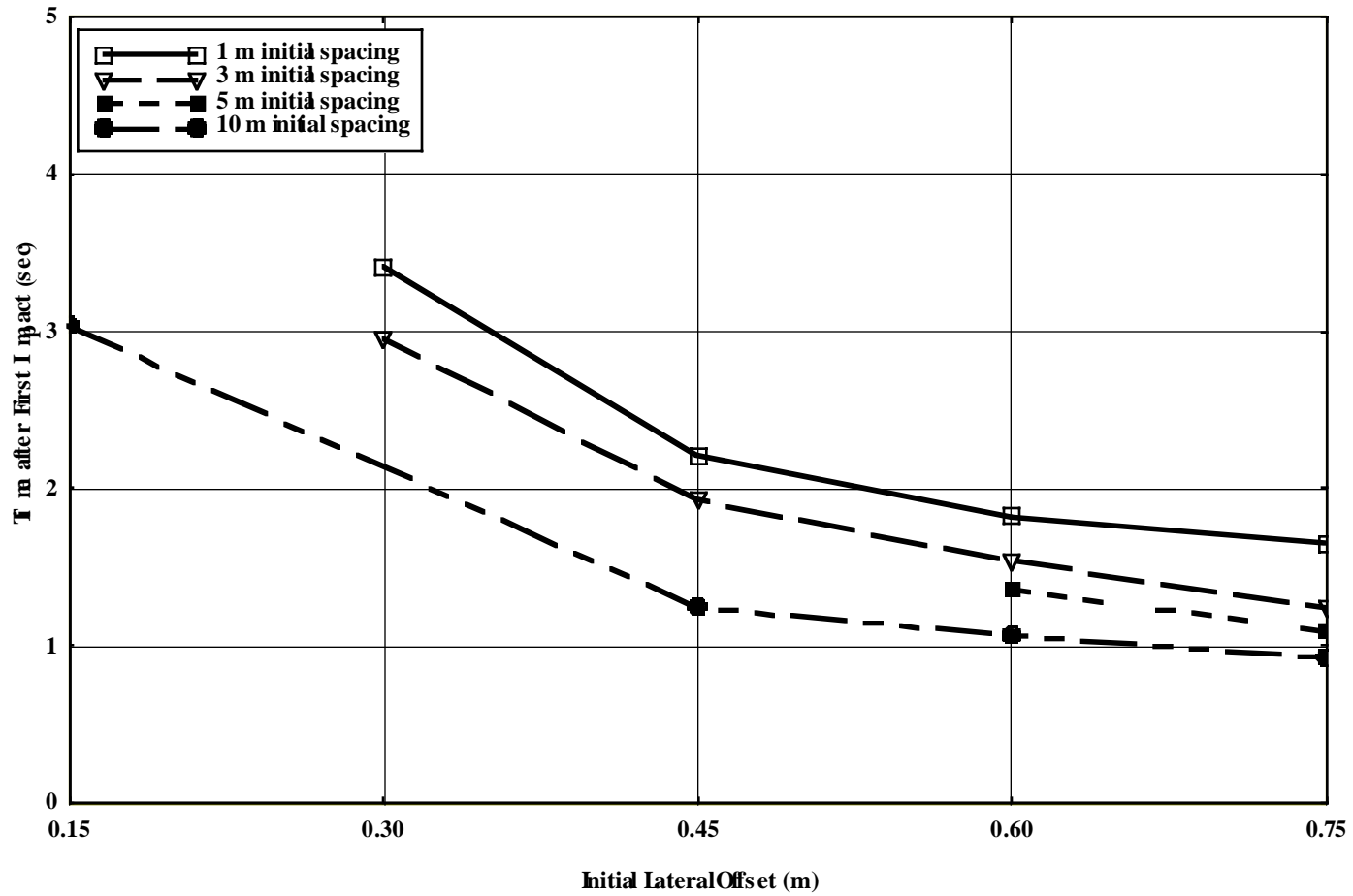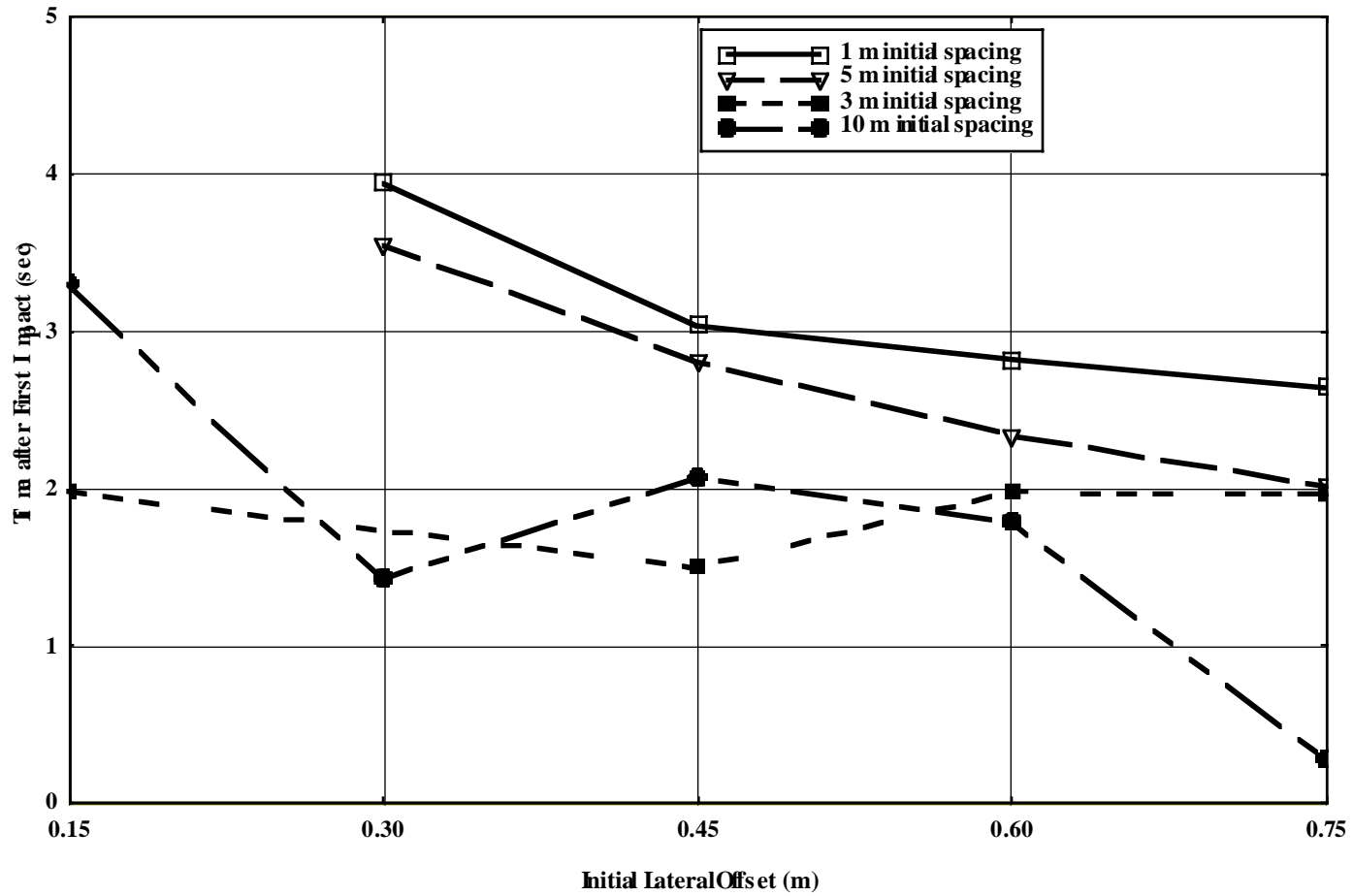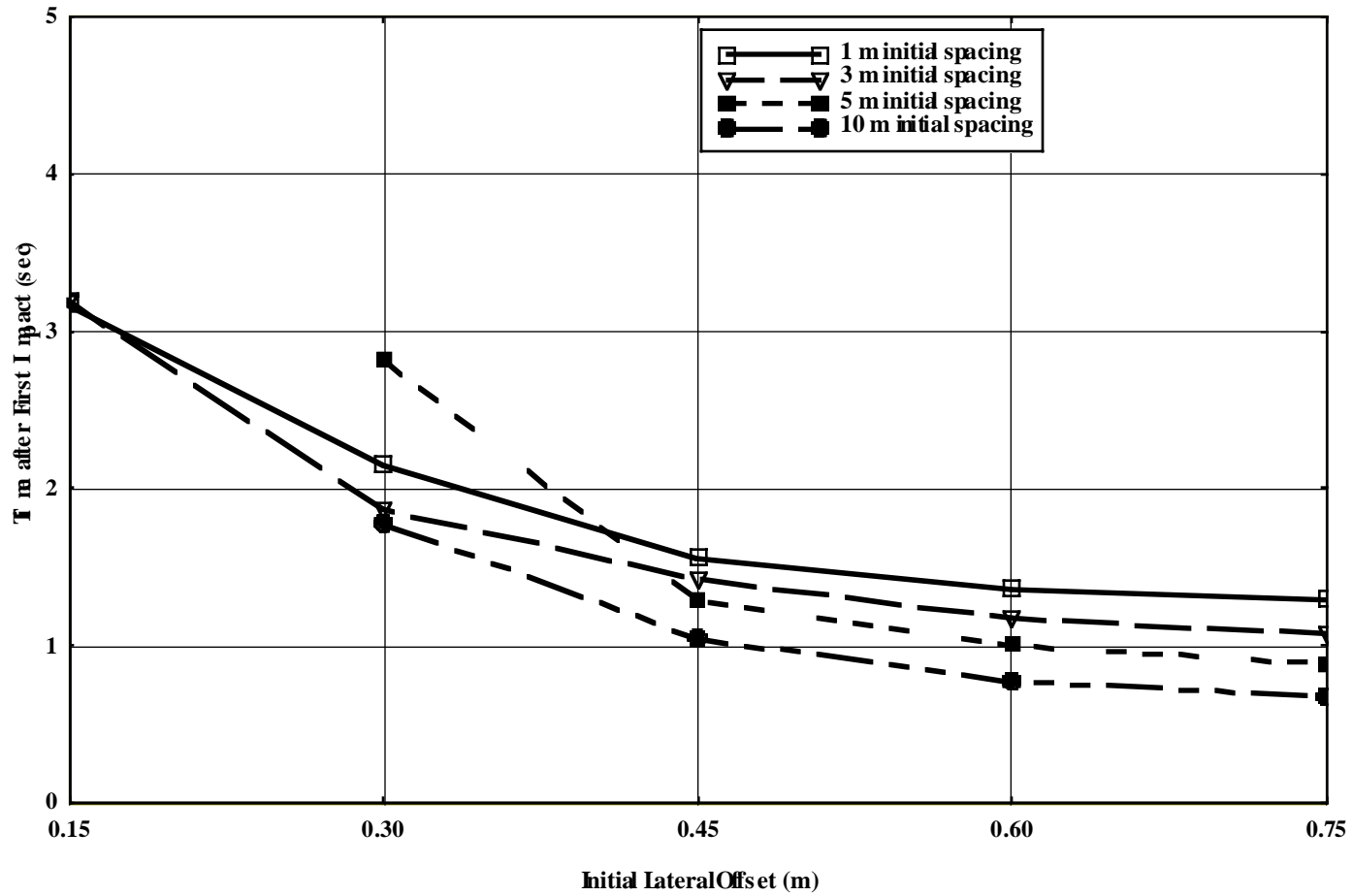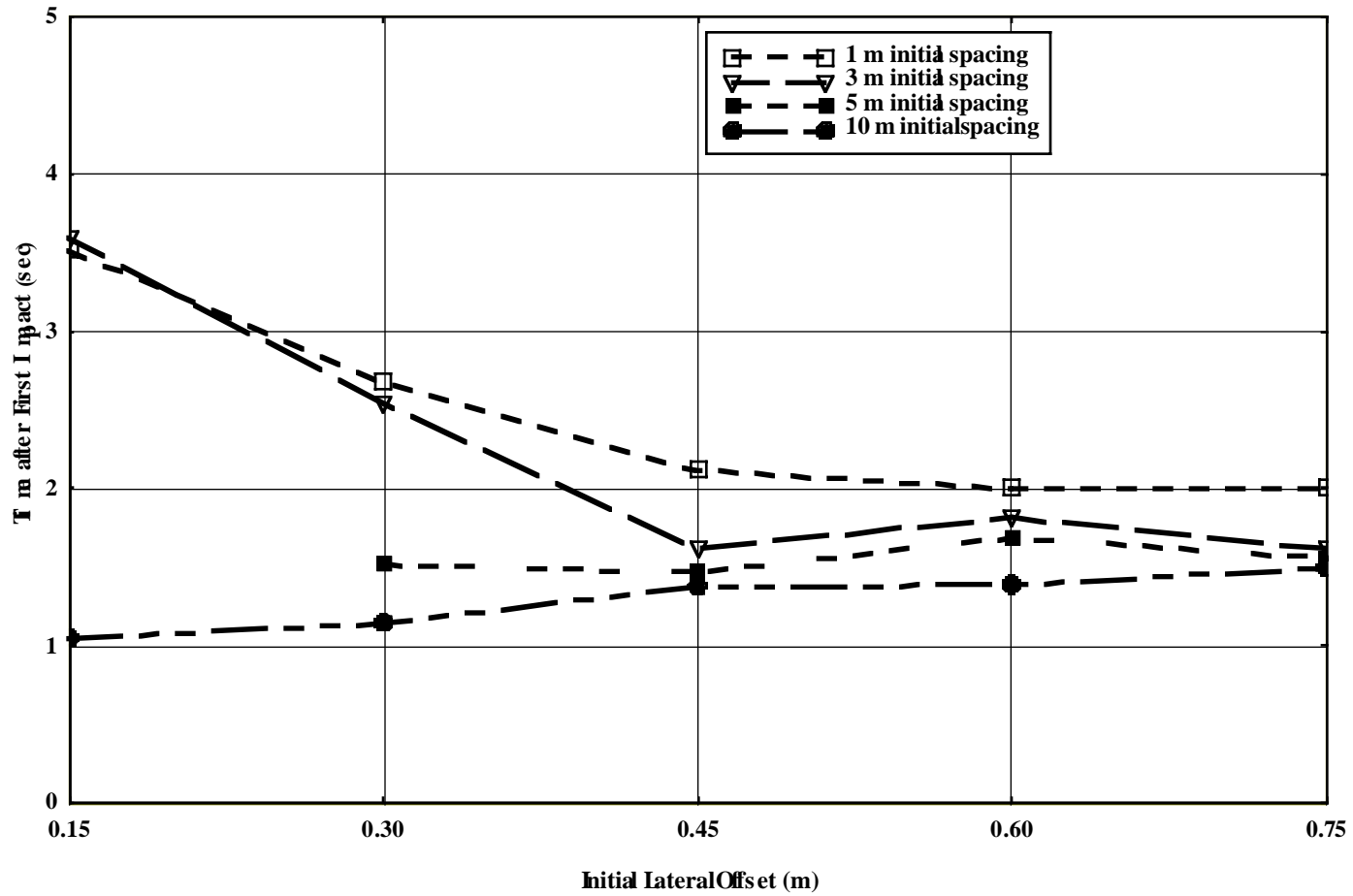
Figure 4. Maximum Lateral Position of Following Vehicle with Class I Leading and Class IV Following for Various Spacing and Lateral Offset
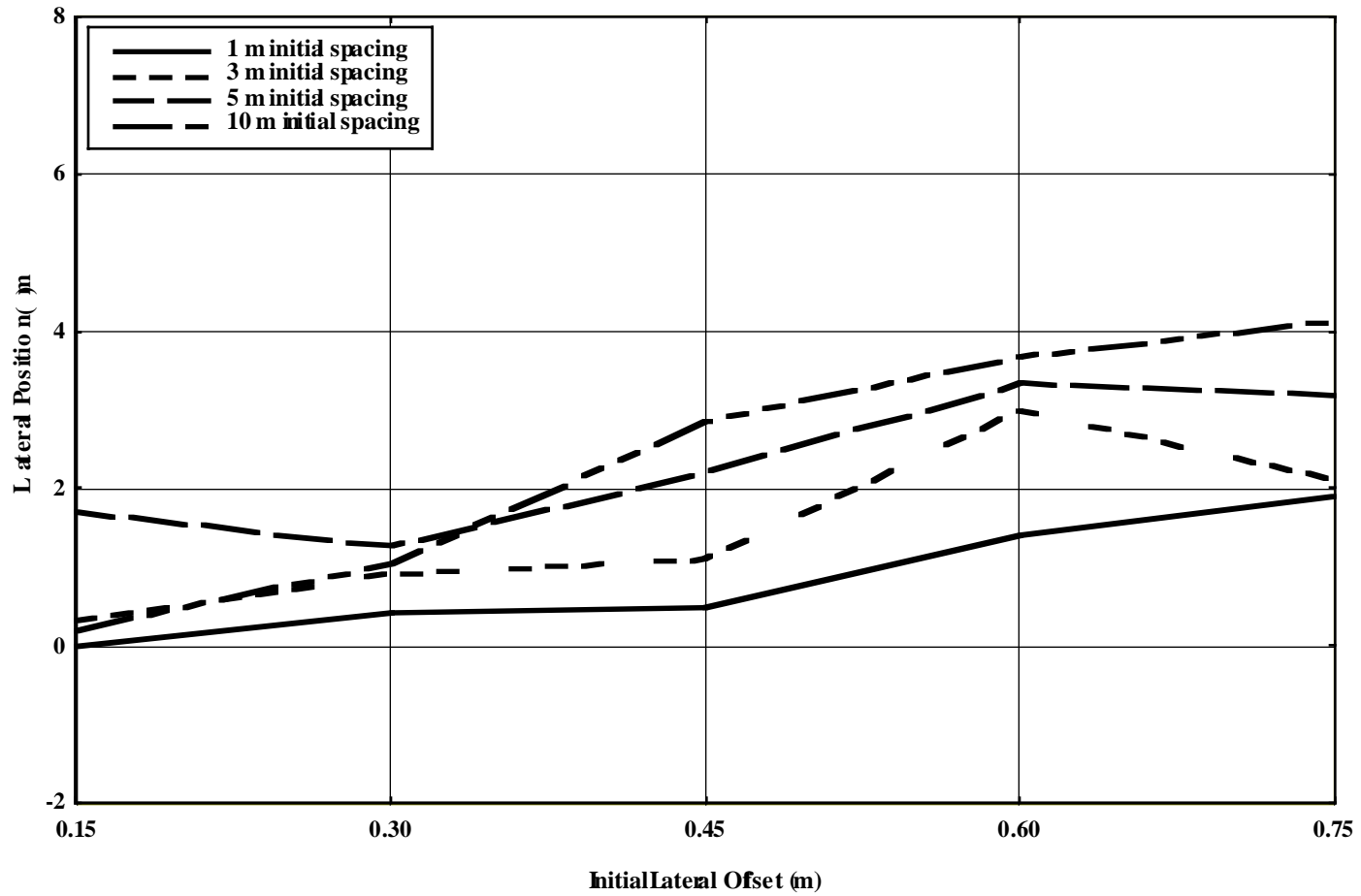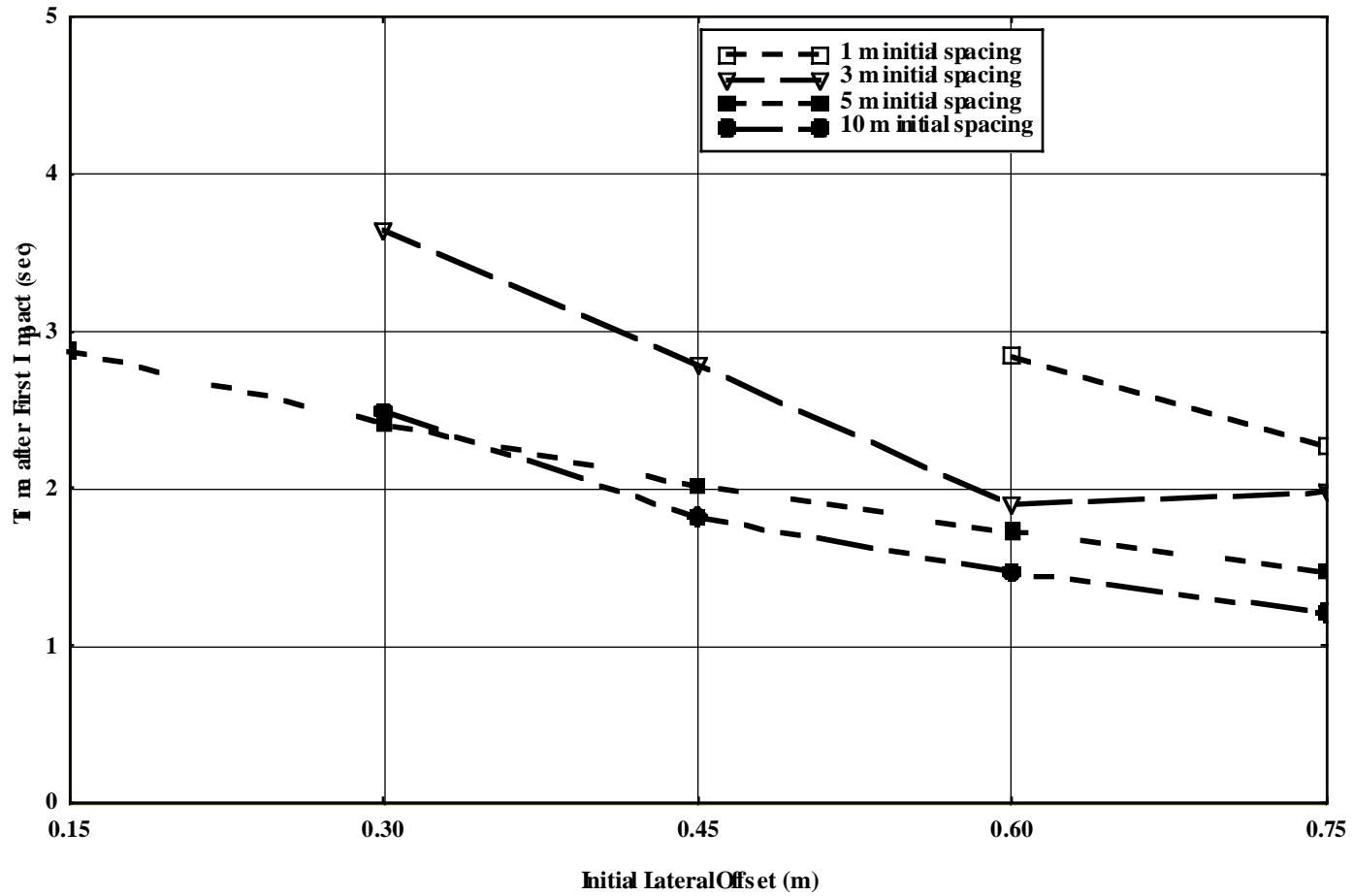
Figure 5. Maximum Lateral Position of Leading Vehicle with Class IV Leading and Class I Following for Various Spacing and Lateral Offset
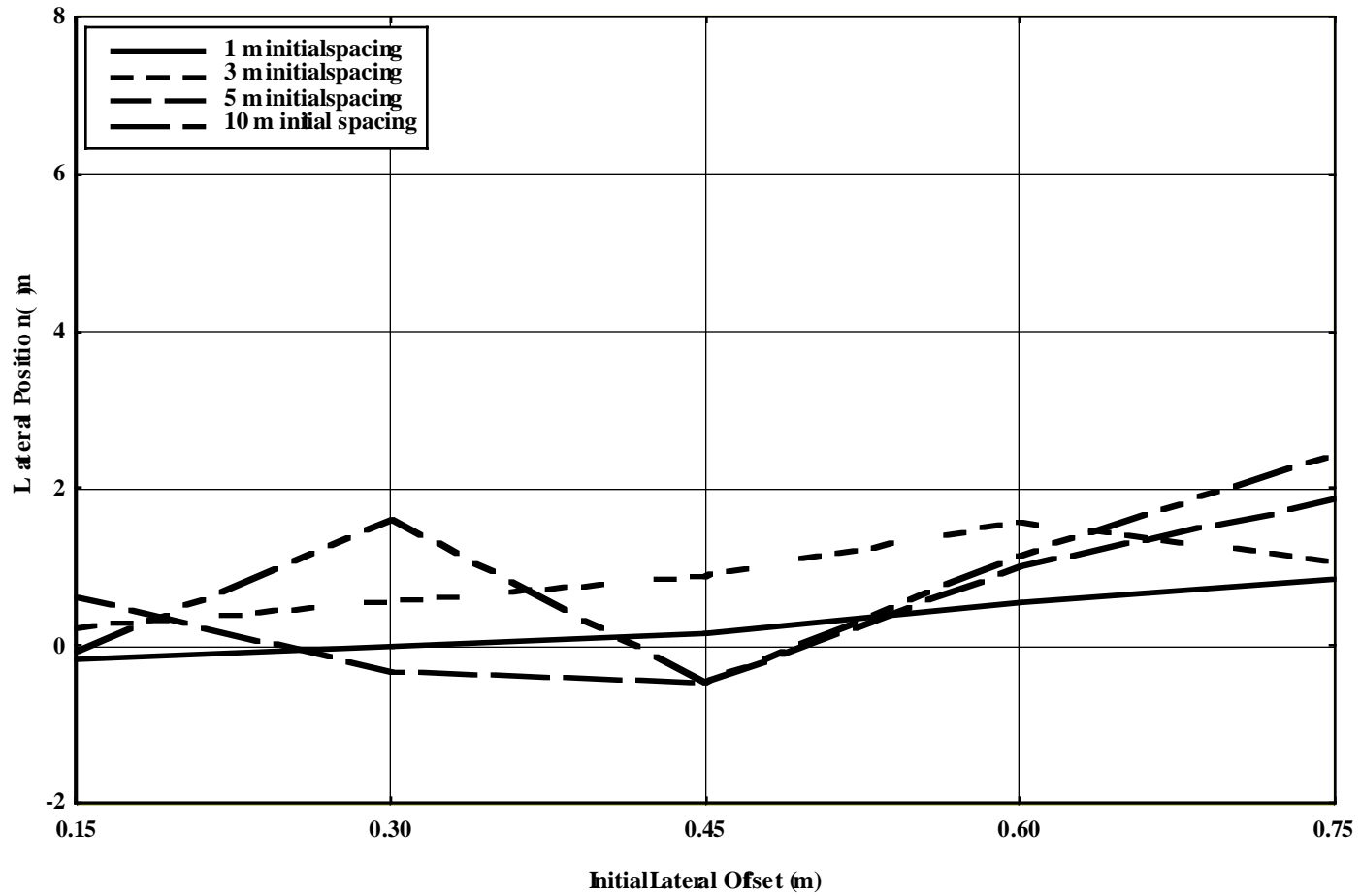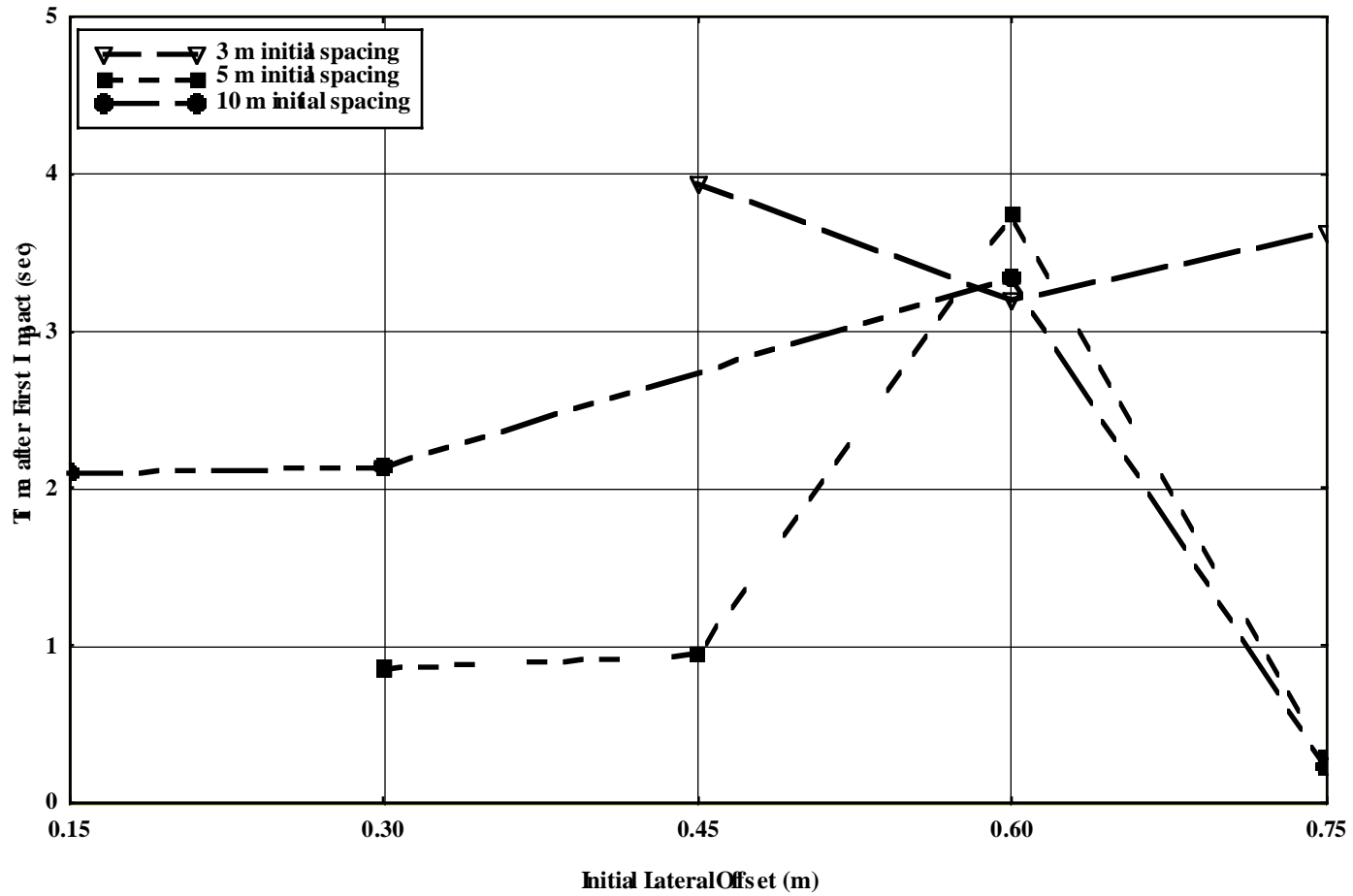
Figure 6. Maximum Lateral Position of Following Vehicle with Class IV Leading and Class I Following for Various Spacing and Lateral Offset
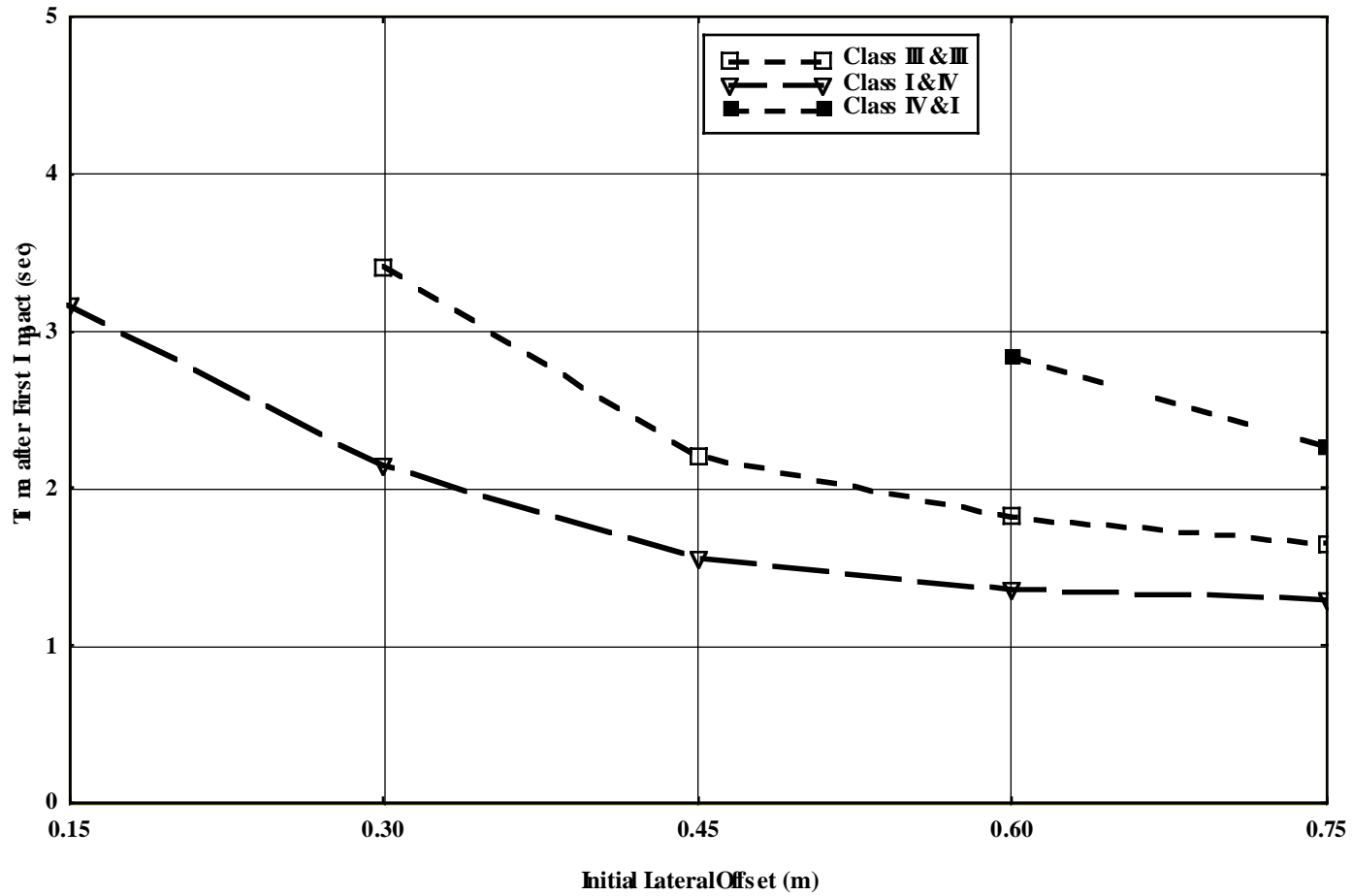
Figure 7. Maximum Lateral Position of Leading Vehicle with 1 m Initial Spacing for Various Formations and Lateral Offset
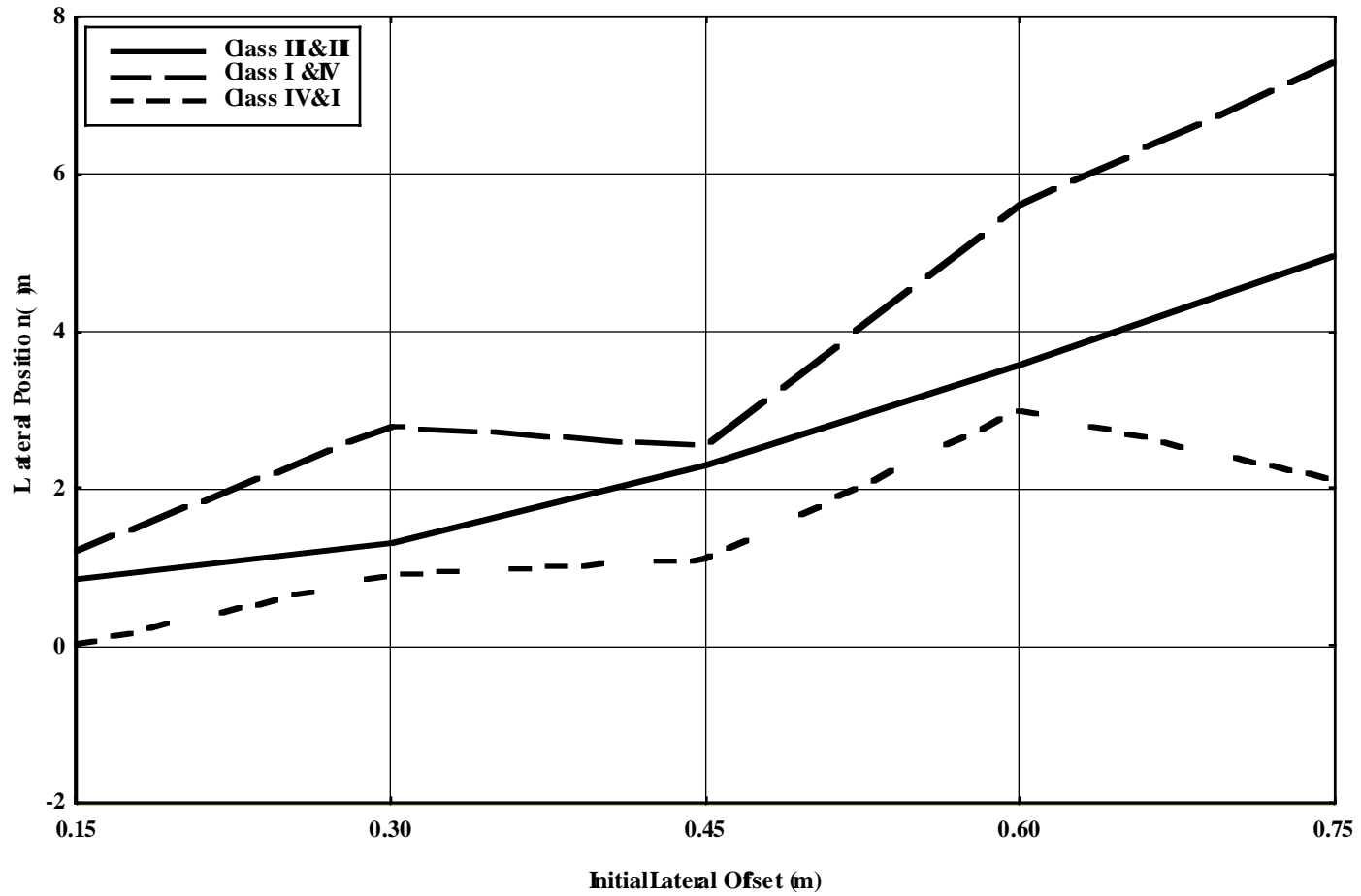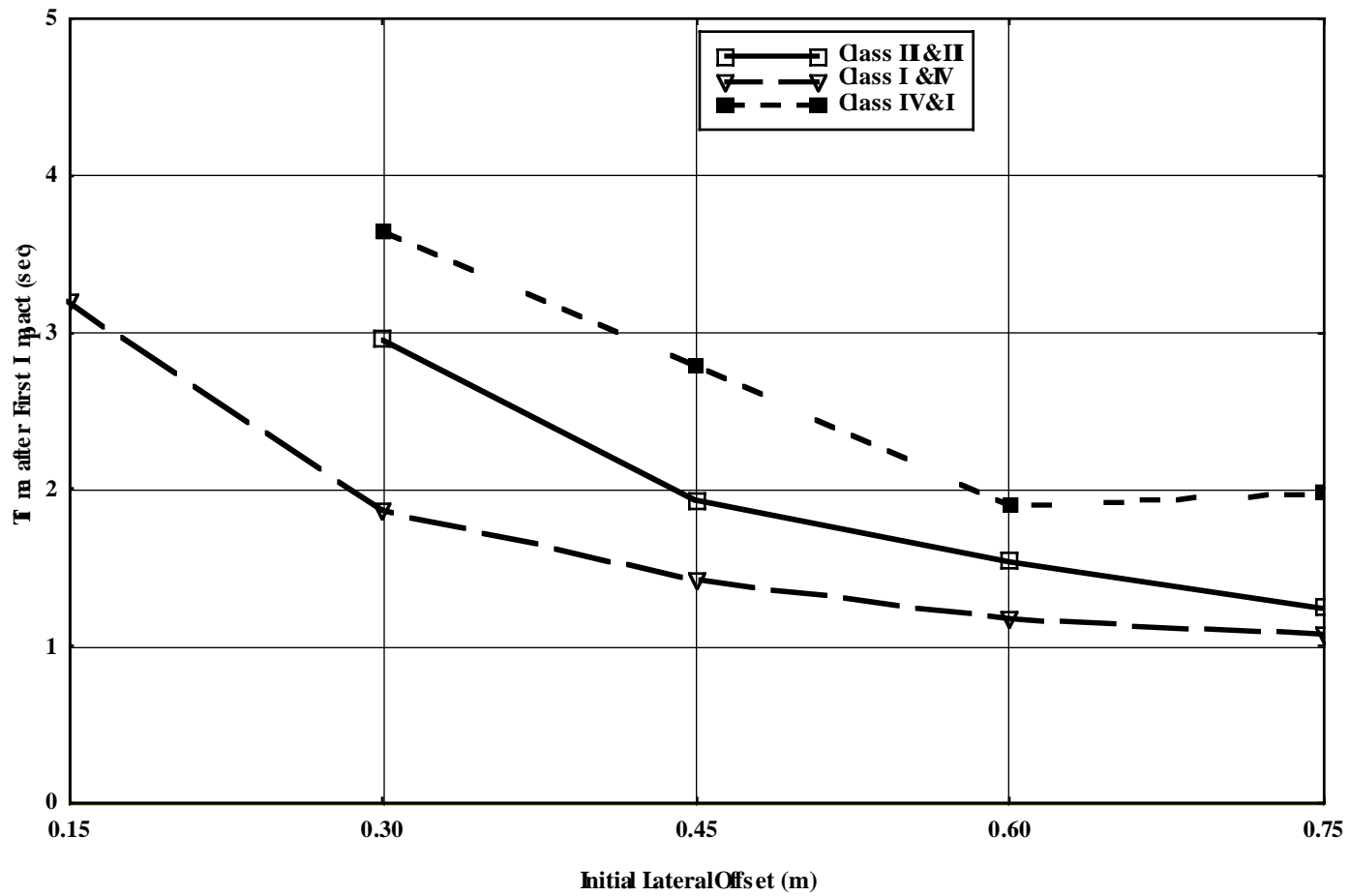
Figure 8. Maximum Lateral Position of Leading Vehicle with 3 m Initial Spacing for Various Formations and Lateral Offset
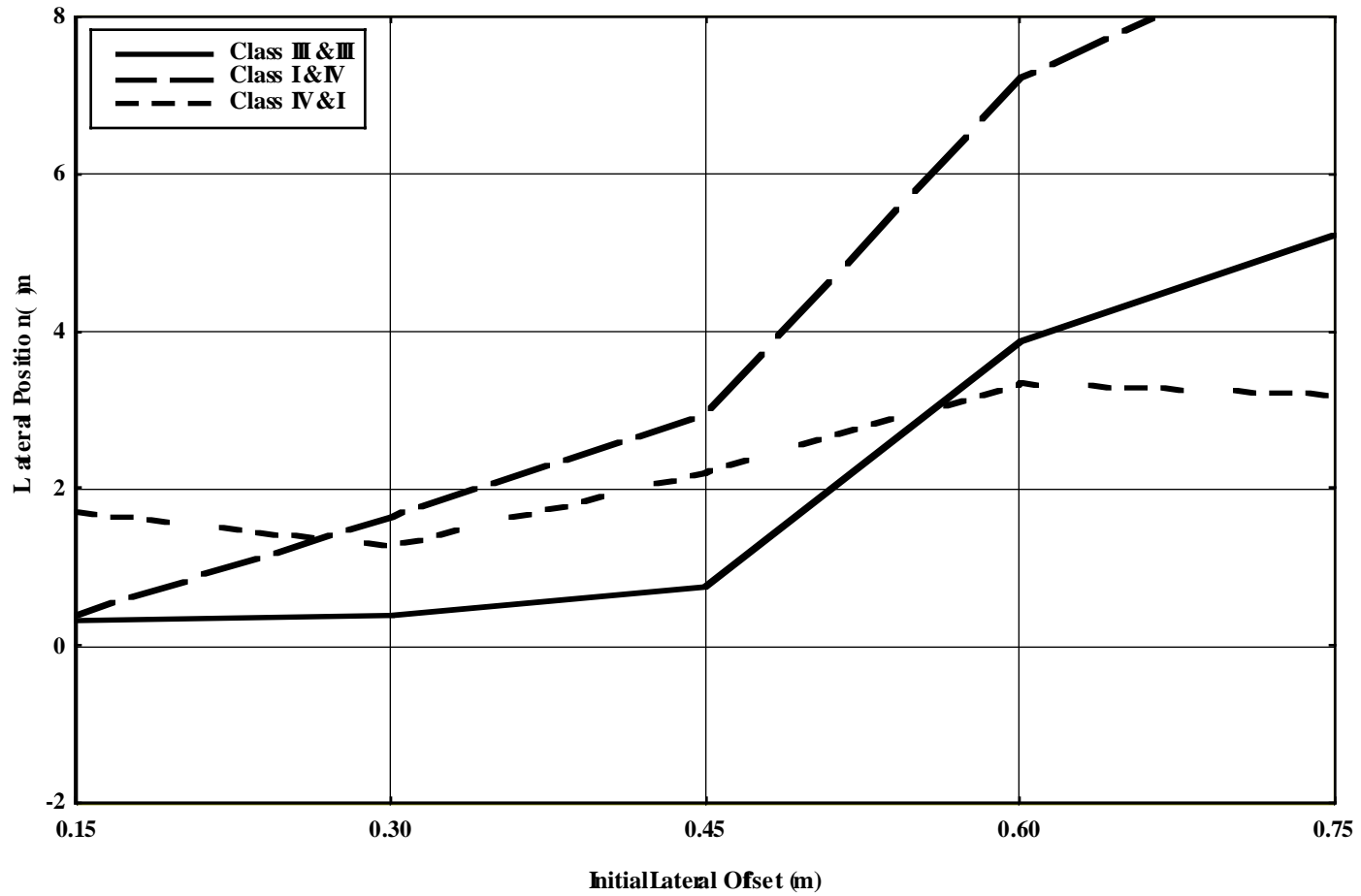
Figure 9. Maximum Lateral Position of Leading Vehicle with 5 m Initial Spacing for Various Formations and Lateral Offset
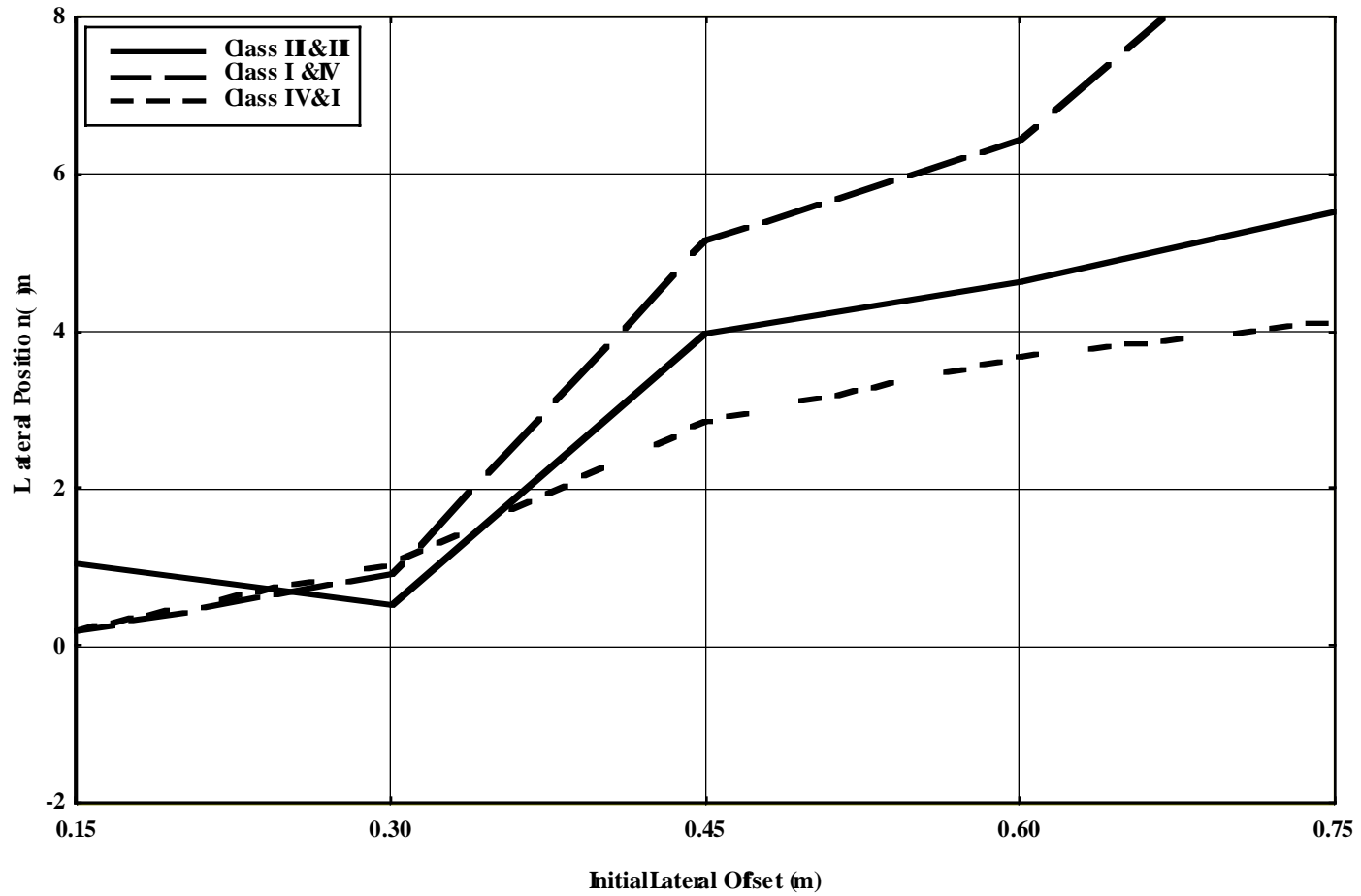
Figure 10. Maximum Lateral Position of Leading Vehicle with 10 m Initial Spacing for Various Formations and Lateral Offset
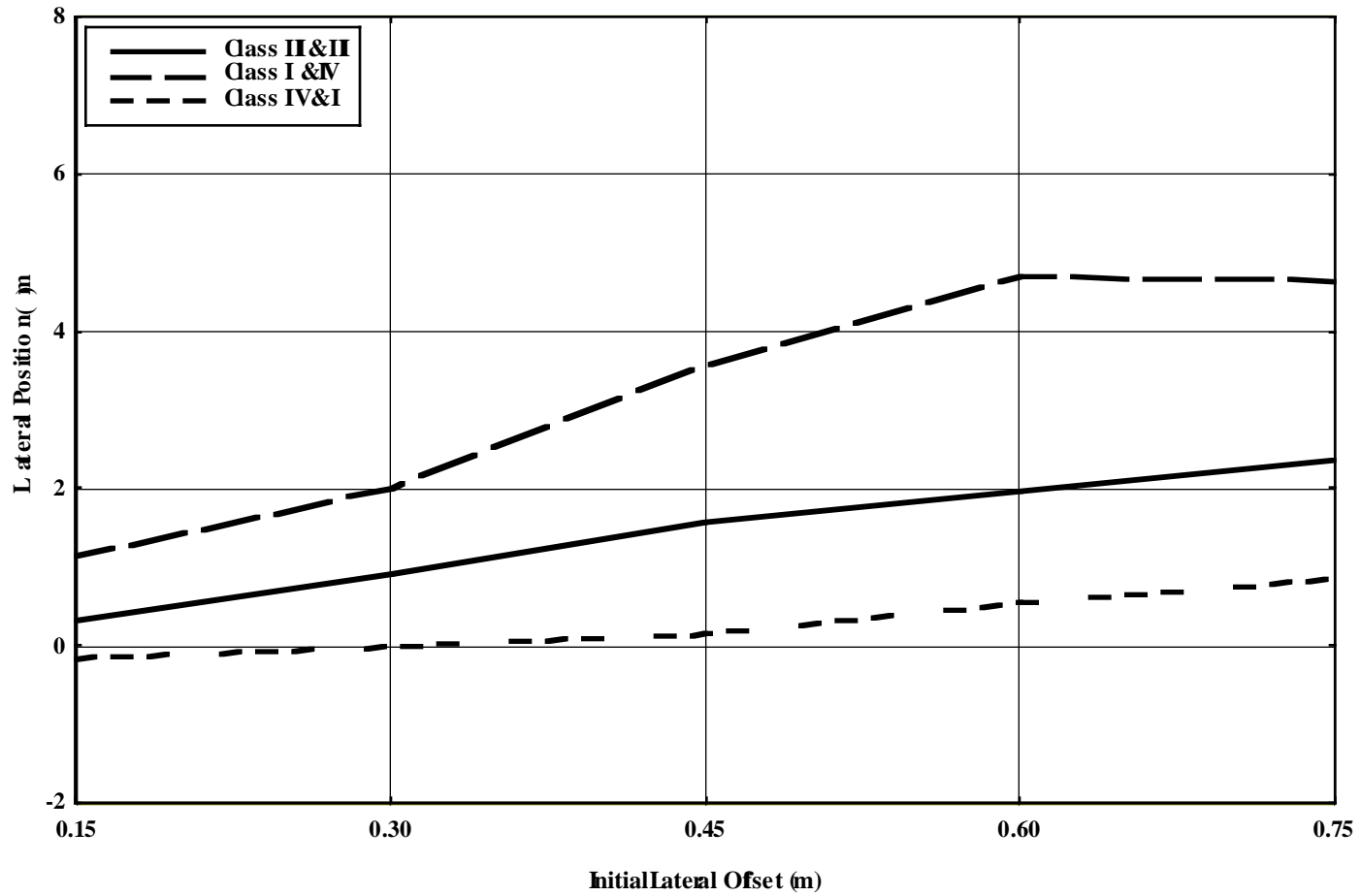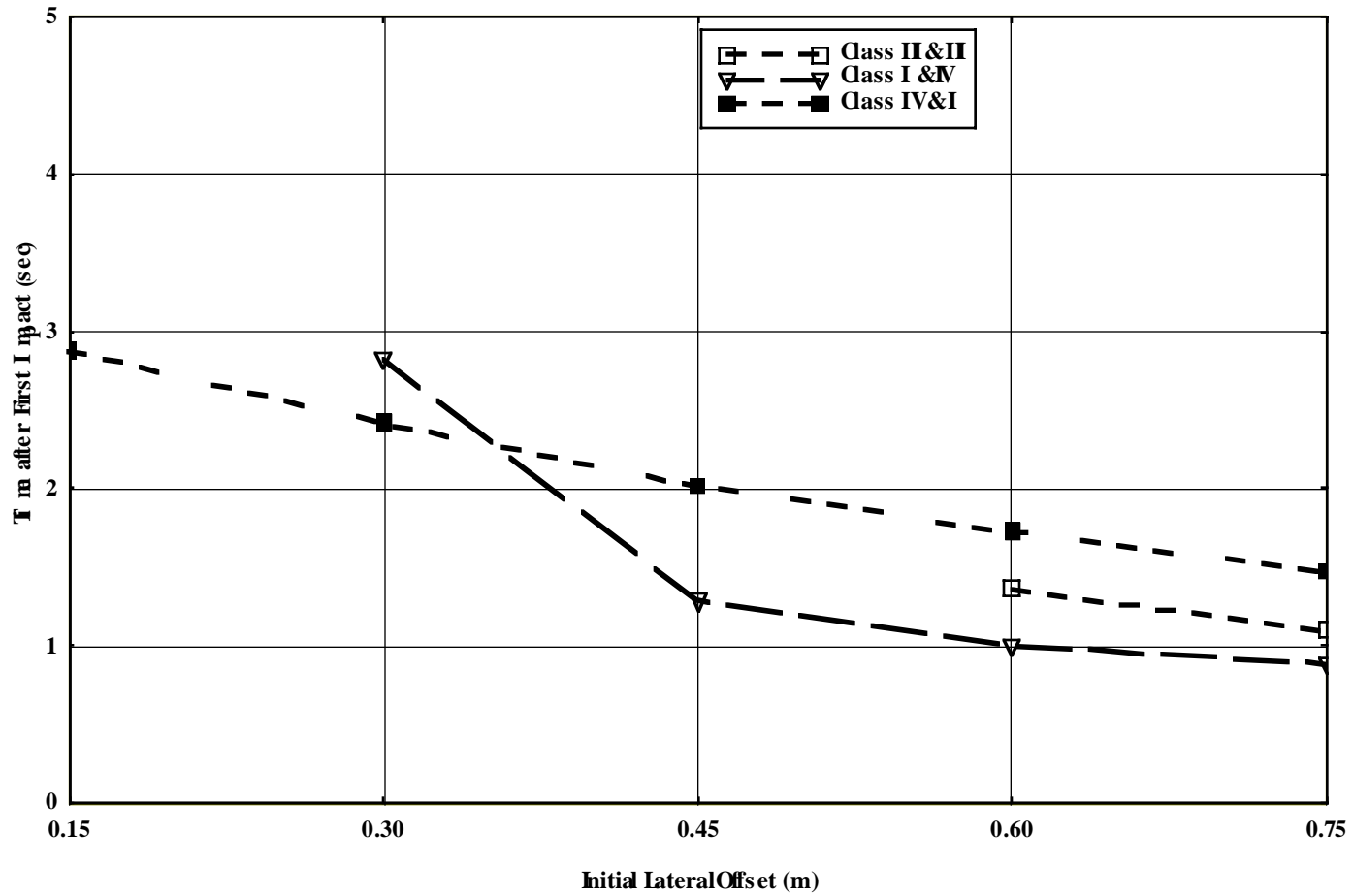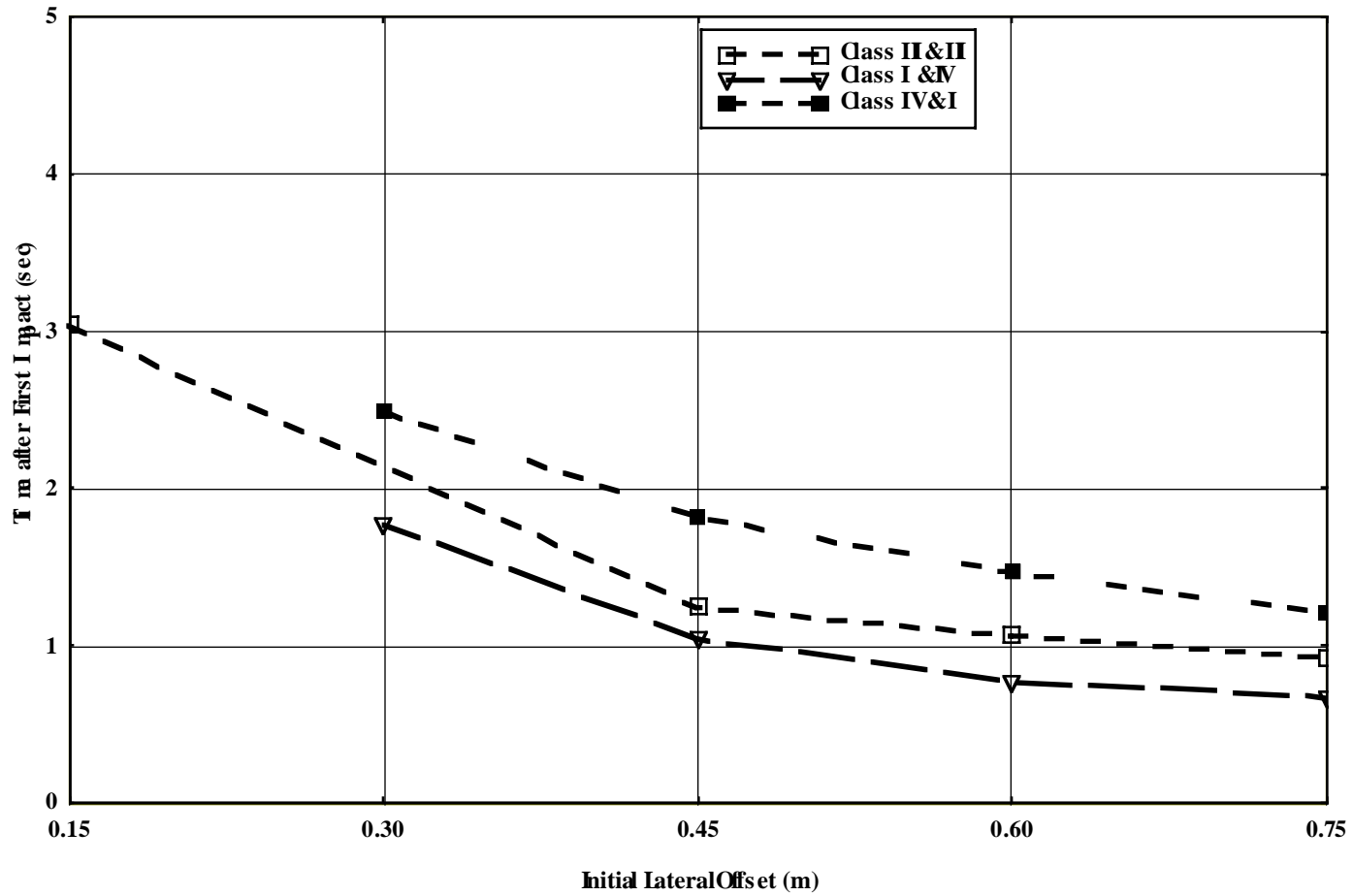
Figure 11. Maximum Lateral Position of Following Vehicle with 1 m Initial Spacing for Various Formations and Lateral Offset
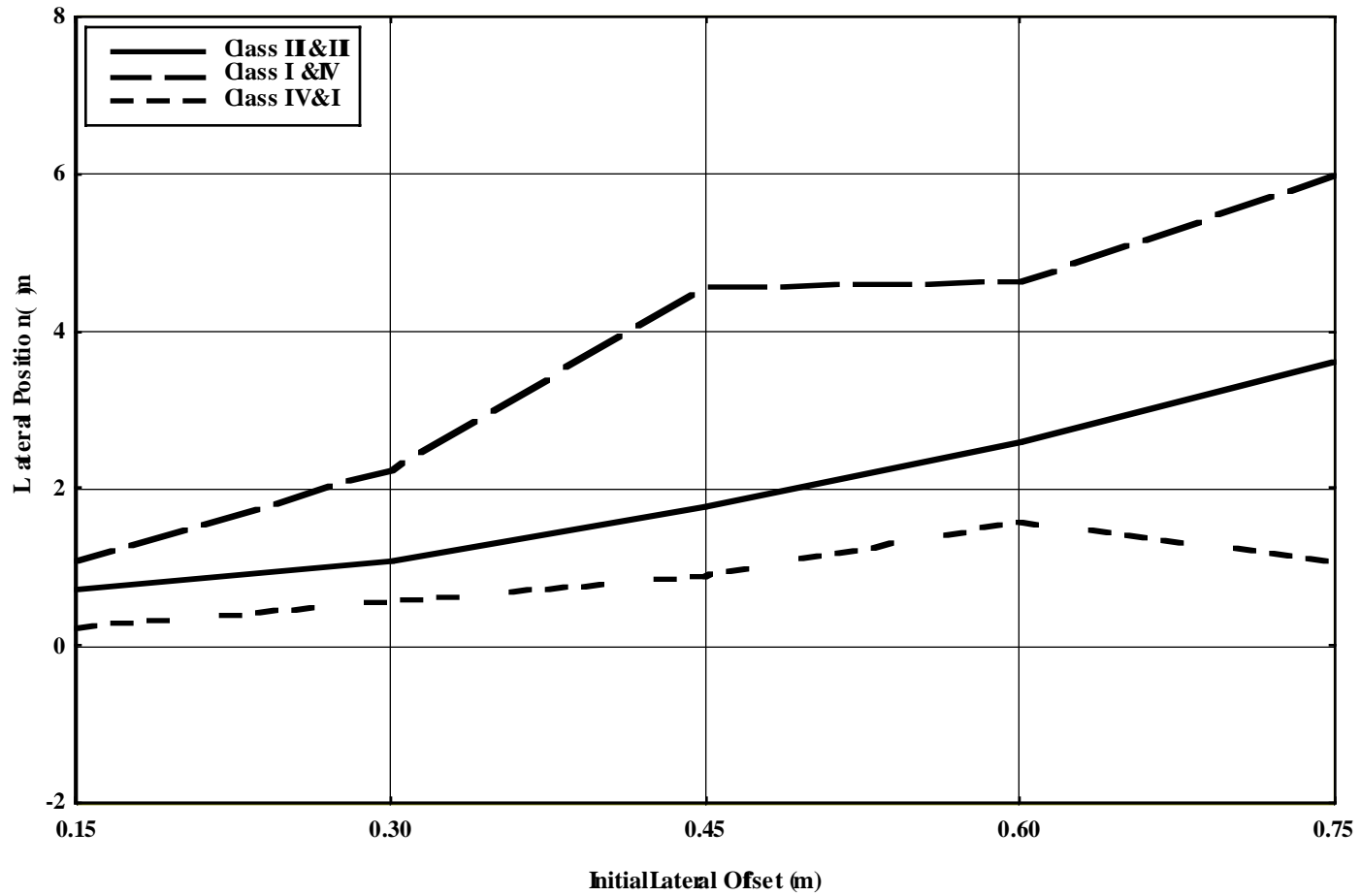
Figure 12. Maximum Lateral Position of Following Vehicle with 3 m Initial Spacing for Various Formations and Lateral Offset
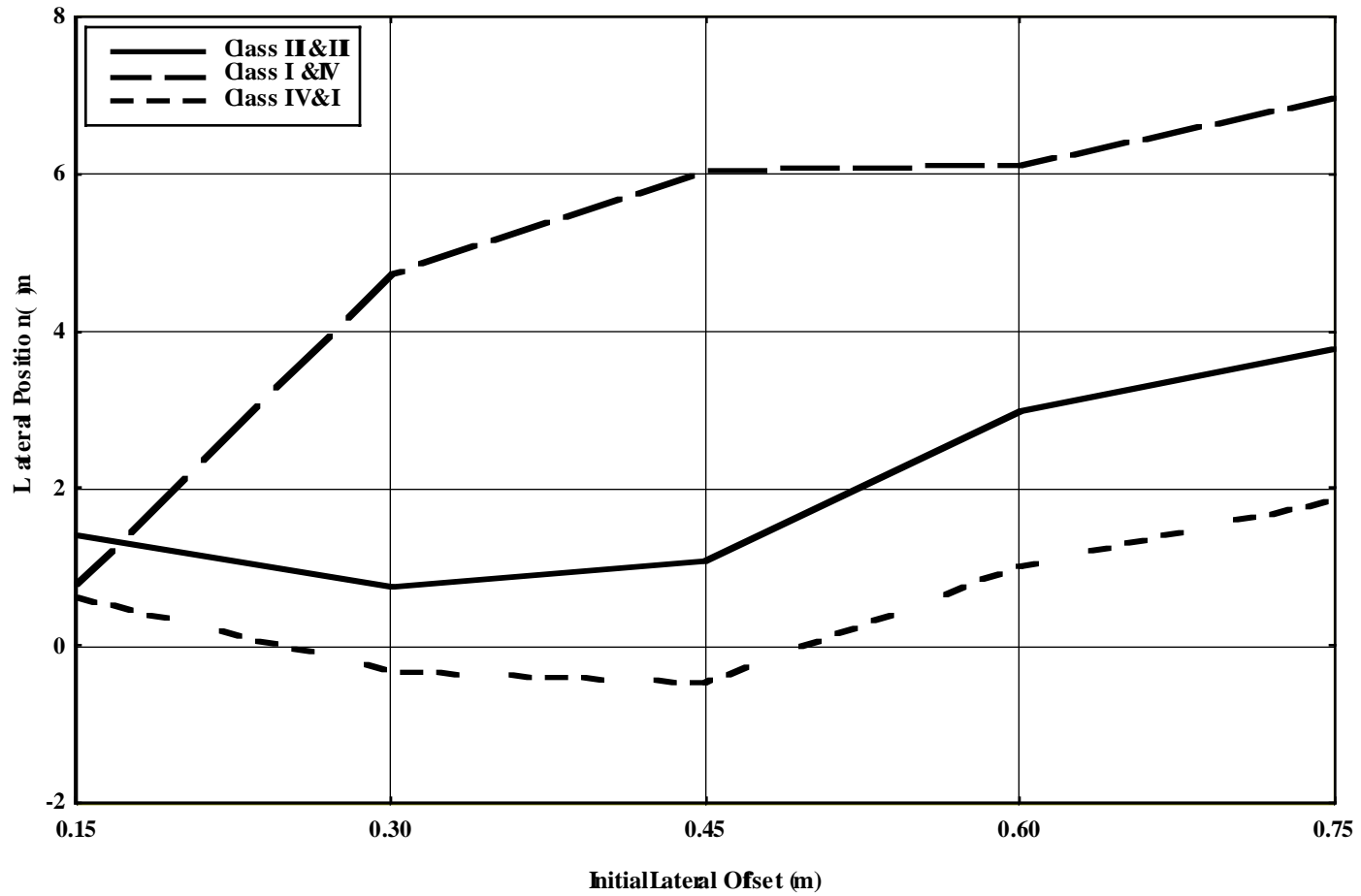
Figure 13. Maximum Lateral Position of Following Vehicle with 5 m Initial Spacing for Various Formations and Lateral Offset
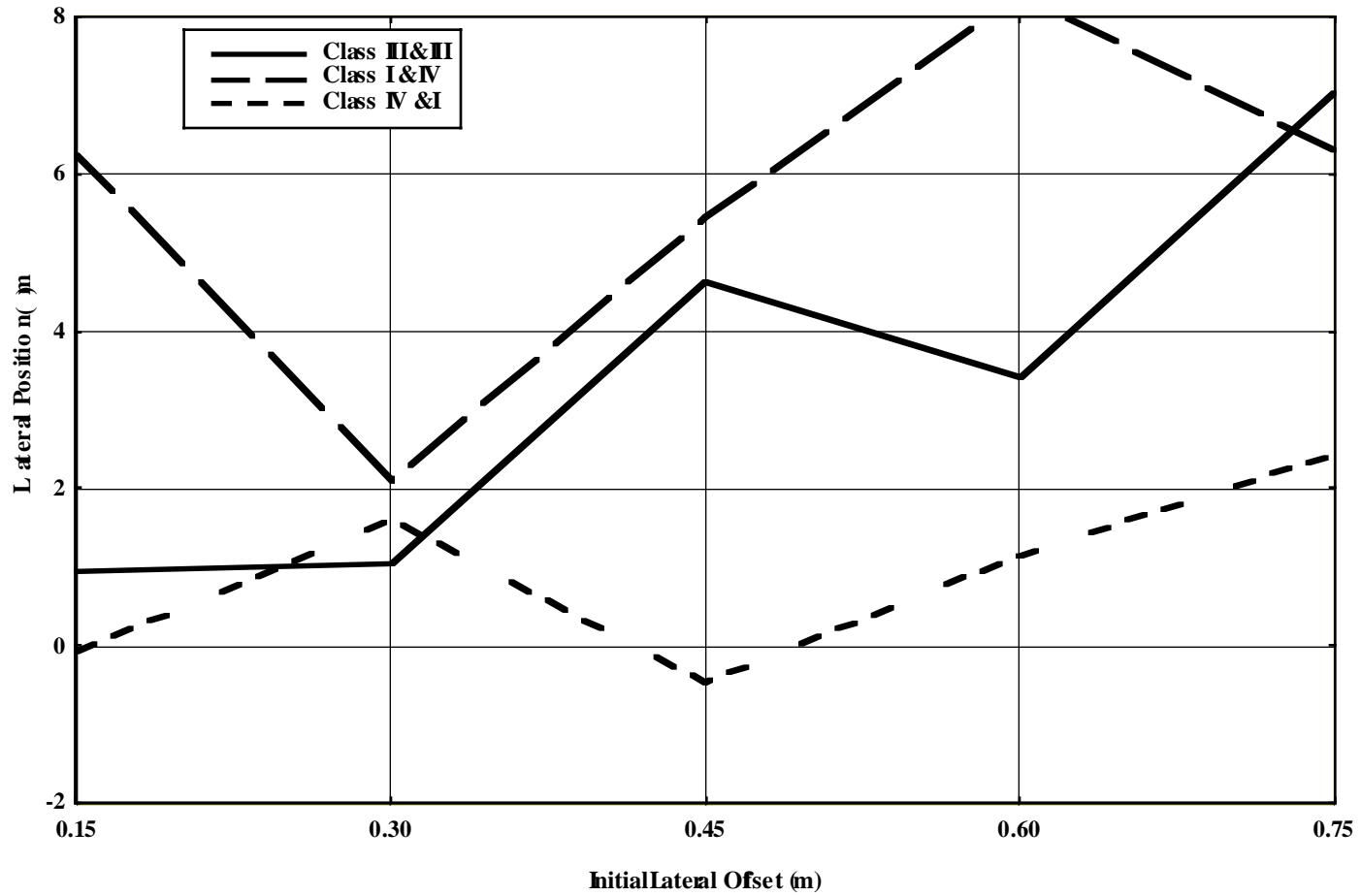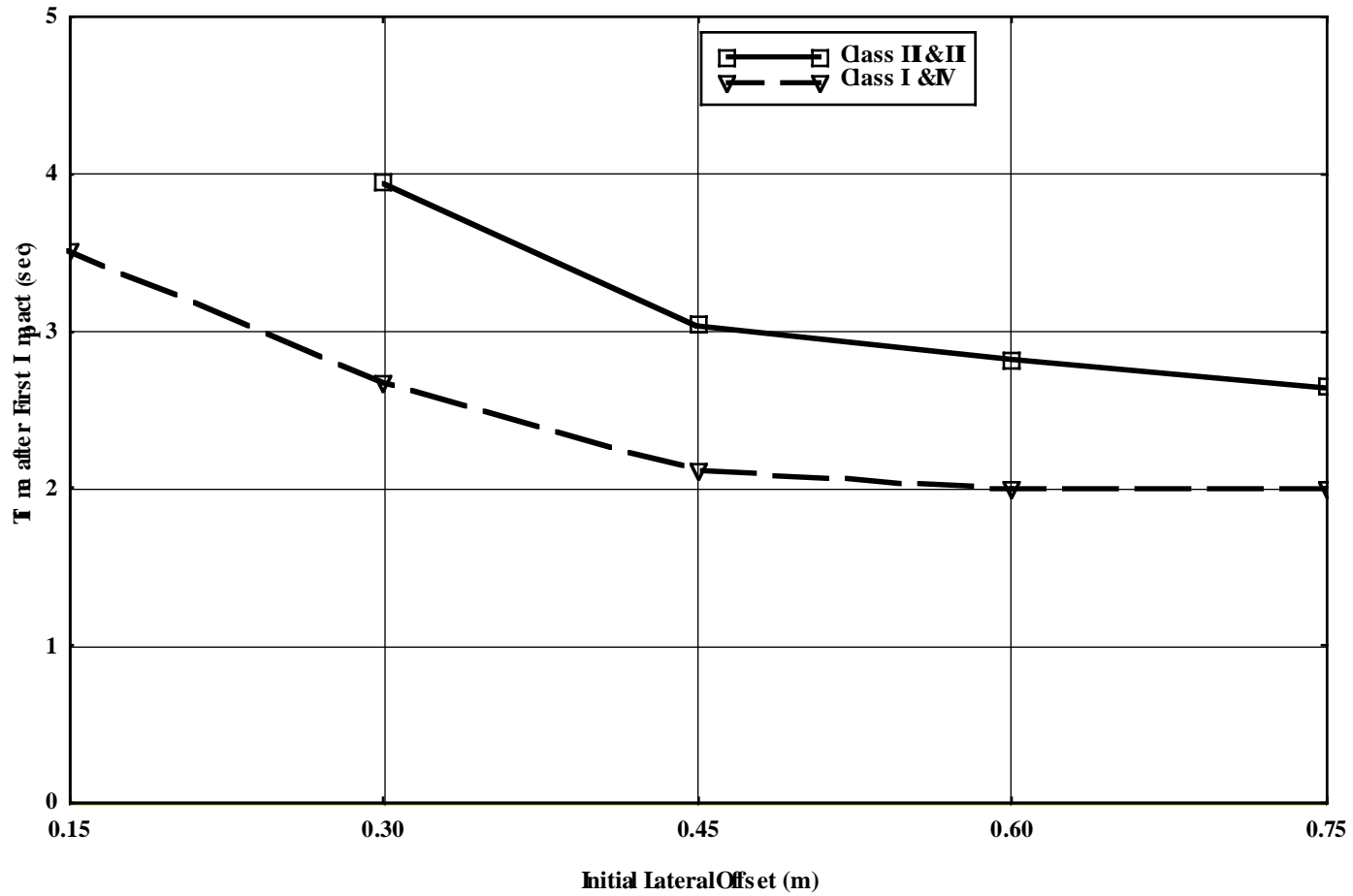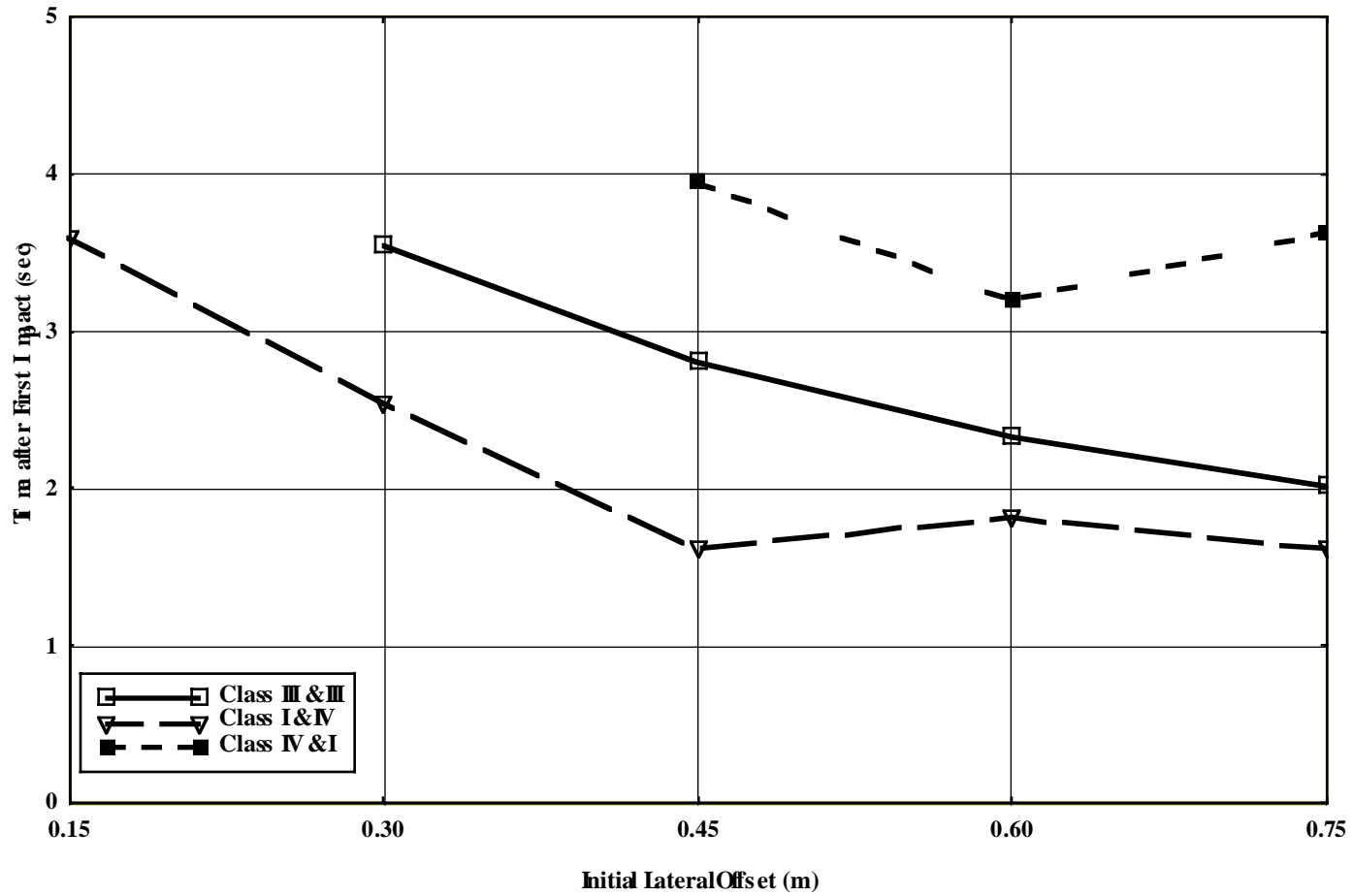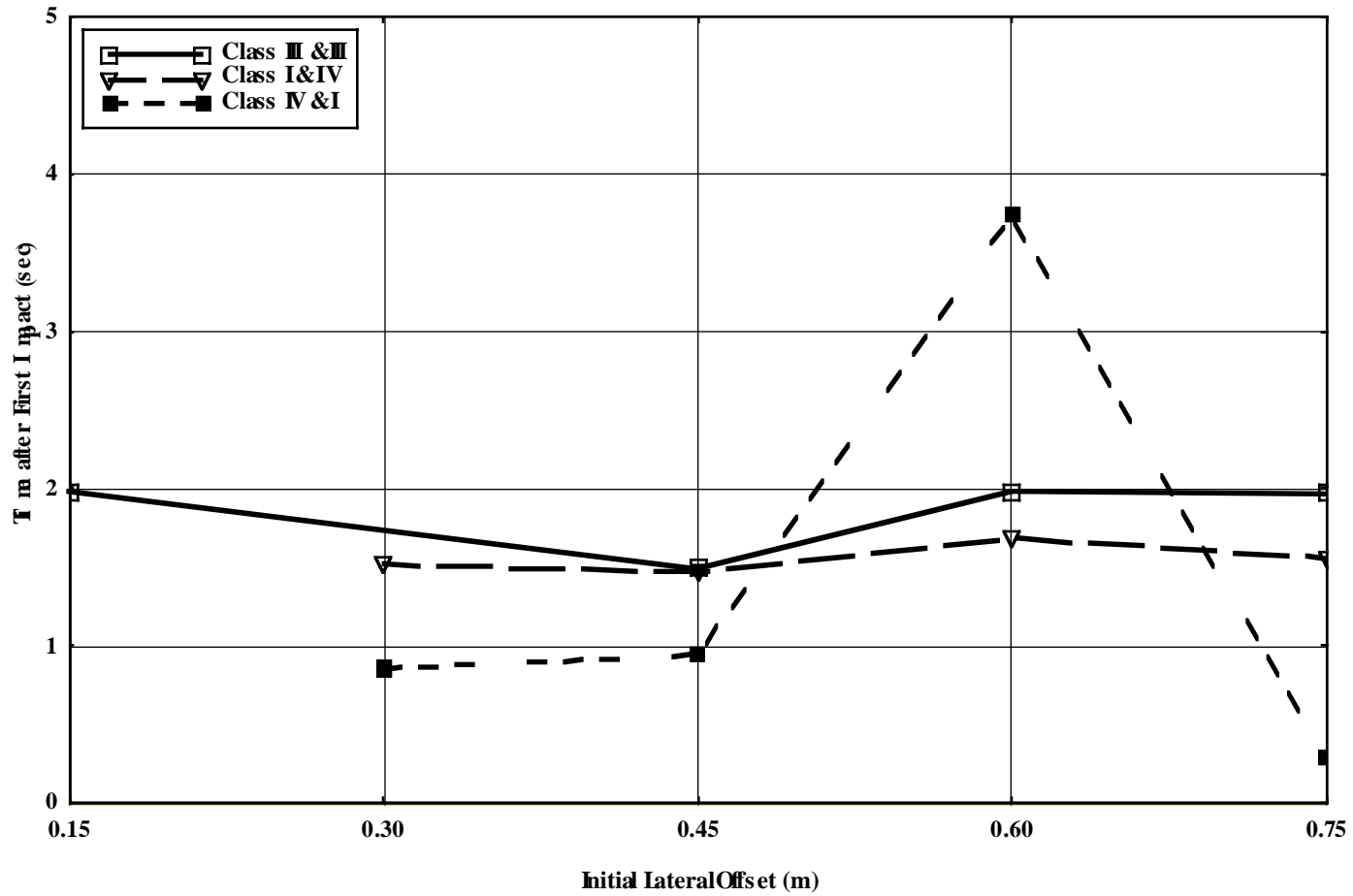
Figure 14. Maximum Lateral Position of Following Vehicle with 10 m Initial Spacing for Various Formations and Lateral Offset
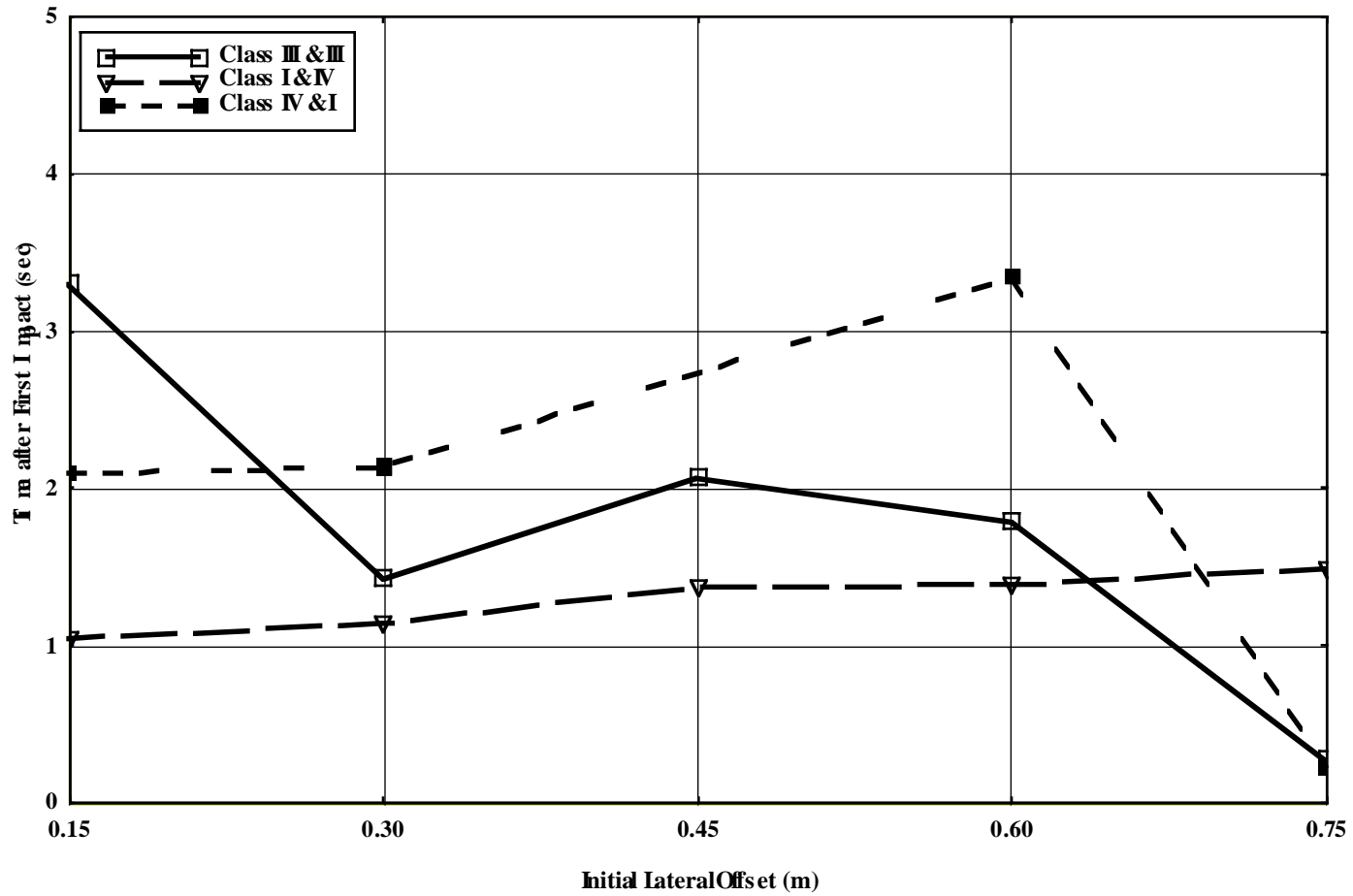
Figure 15. Lane Departure Time of Leading Vehicle with Class III Leading and Class III Following for Various Spacing and Lateral Offset

Figure 16. Lane Departure Time of Following Vehicle with Class III Leading and Class III Following for Various Spacing and Lateral Offset

Figure 17. Lane Departure Time of Leading Vehicle with Class I Leading and Class IV Following for Various Spacing and Lateral Offset

Figure 18. Lane Departure Time of Following Vehicle with Class I Leading and Class IV Following for Various Spacing and Lateral Offset

Figure 19. Lane Departure Time of Leading Vehicle with Class IV Leading and Class I Following for Various Spacing and Lateral Offset

Figure 20. Lane Departure Time of Following Vehicle with Class IV Leading and Class I Following for Various Spacing and Lateral Offset

Figure 21. Lane Departure Time of Leading Vehicle with 1 m Initial Spacing for Various Formations and Lateral Offset

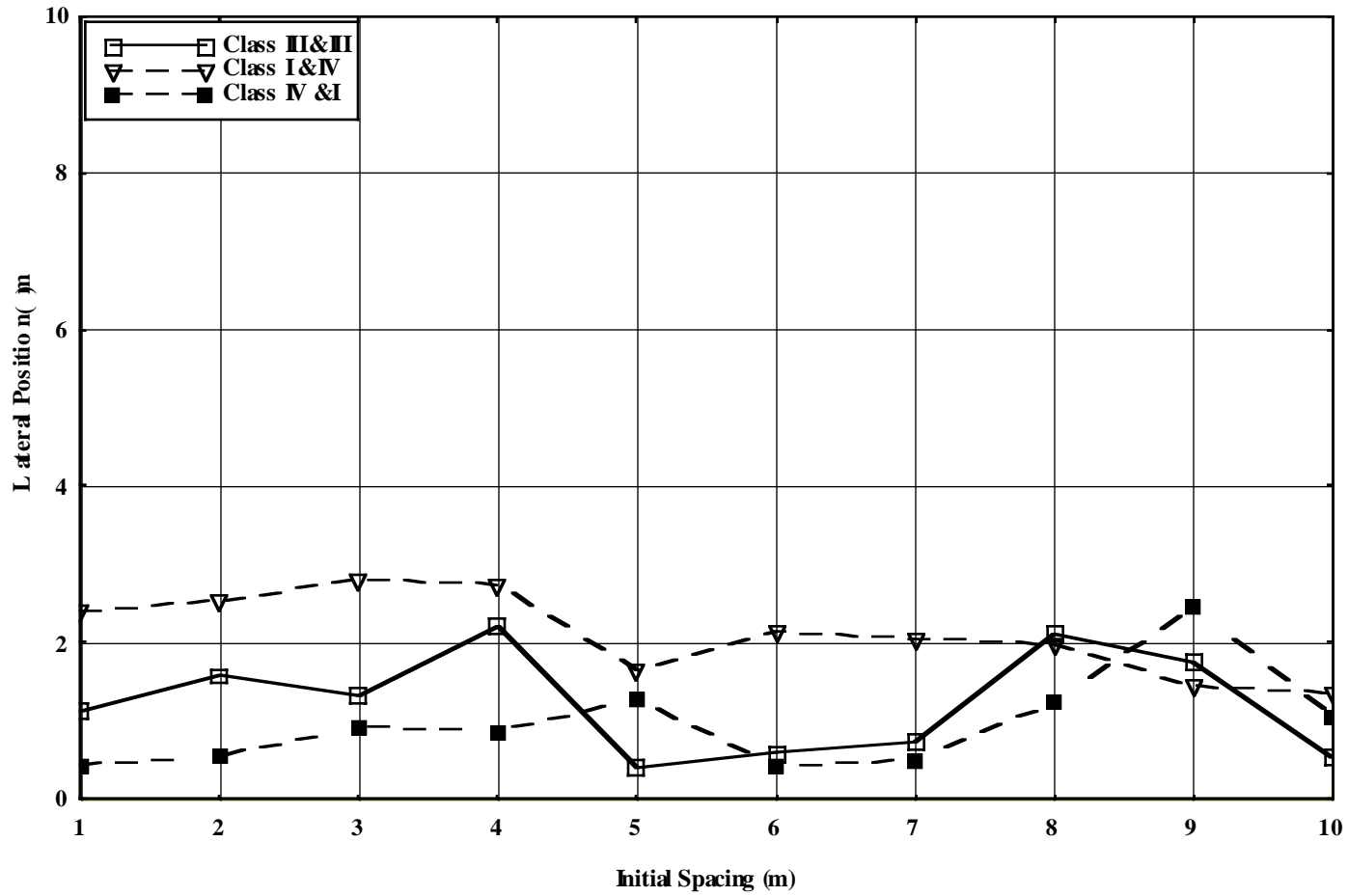Figure 22. Lane Departure Time of Leading Vehicle with 3 m Initial Spacing for Various Formations and Lateral Offset

Figure 23. Lane Departure Time of Leading Vehicle with 5 m Initial Spacing for Various Formations and Lateral Offset

Figure 24. Lane Departure Time of Leading Vehicle with 10 m Initial Spacing for Various Formations and Lateral Offset

Figure 25. Lane Departure Time of Following Vehicle with 1 m Initial Spacing for Various Formations and Lateral Offset

Figure 26. Lane Departure Time of Following Vehicle with 3 m Initial Spacing for Various Formations and Lateral Offset

Figure 27. Lane Departure Time of Following Vehicle with 5 m Initial Spacing for Various Formations and Lateral Offset

Figure 28. Lane Departure Time of Following Vehicle with 10 m Initial Spacing for Various Formations and Lateral Offset

Figure 29. Maximum Abs(Lateral Position) of Leading Vehicle with 105 kmph Initial Speed and 0.3 m Lateral Offset for Various Formations and Initial Spacing
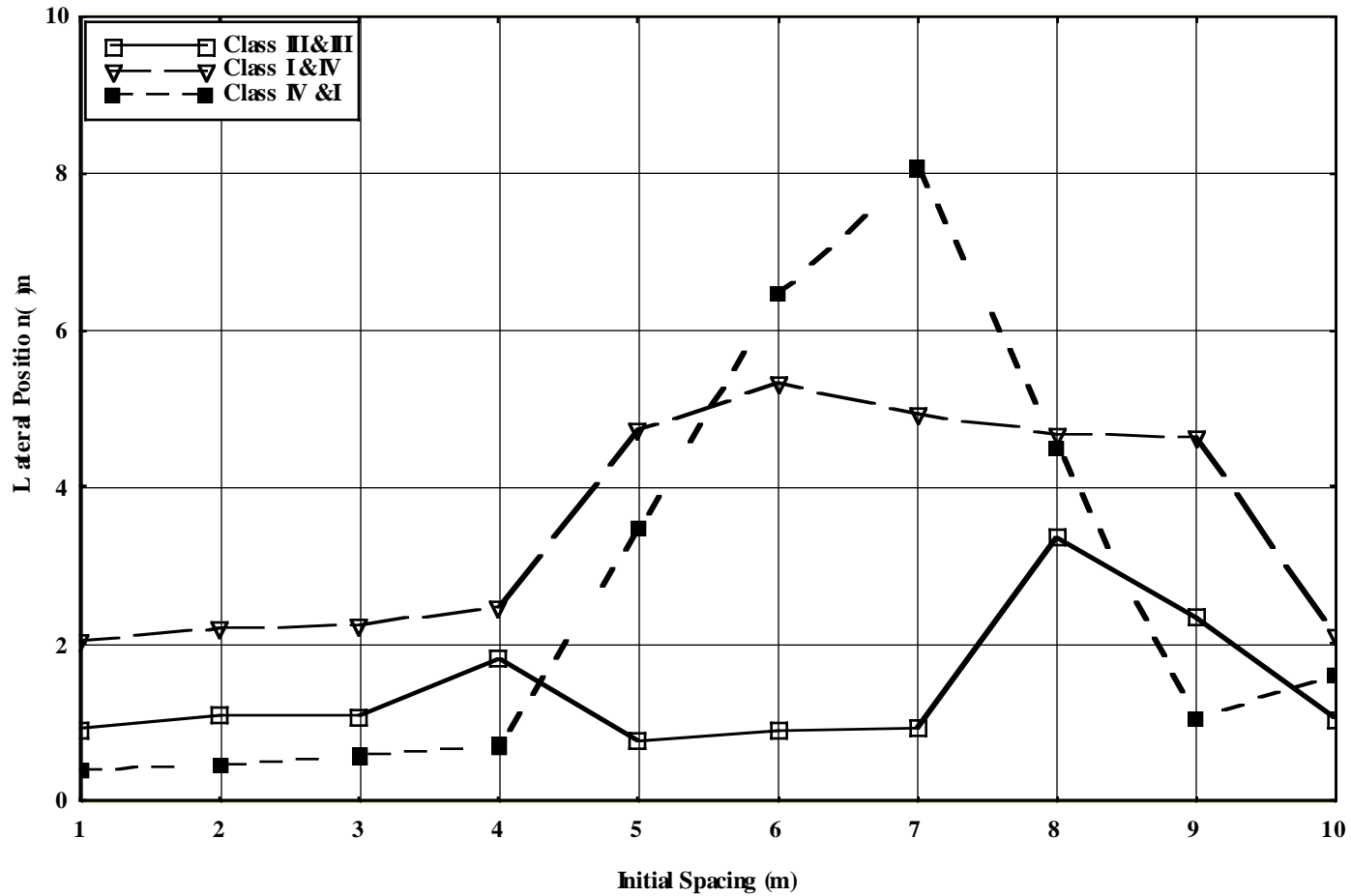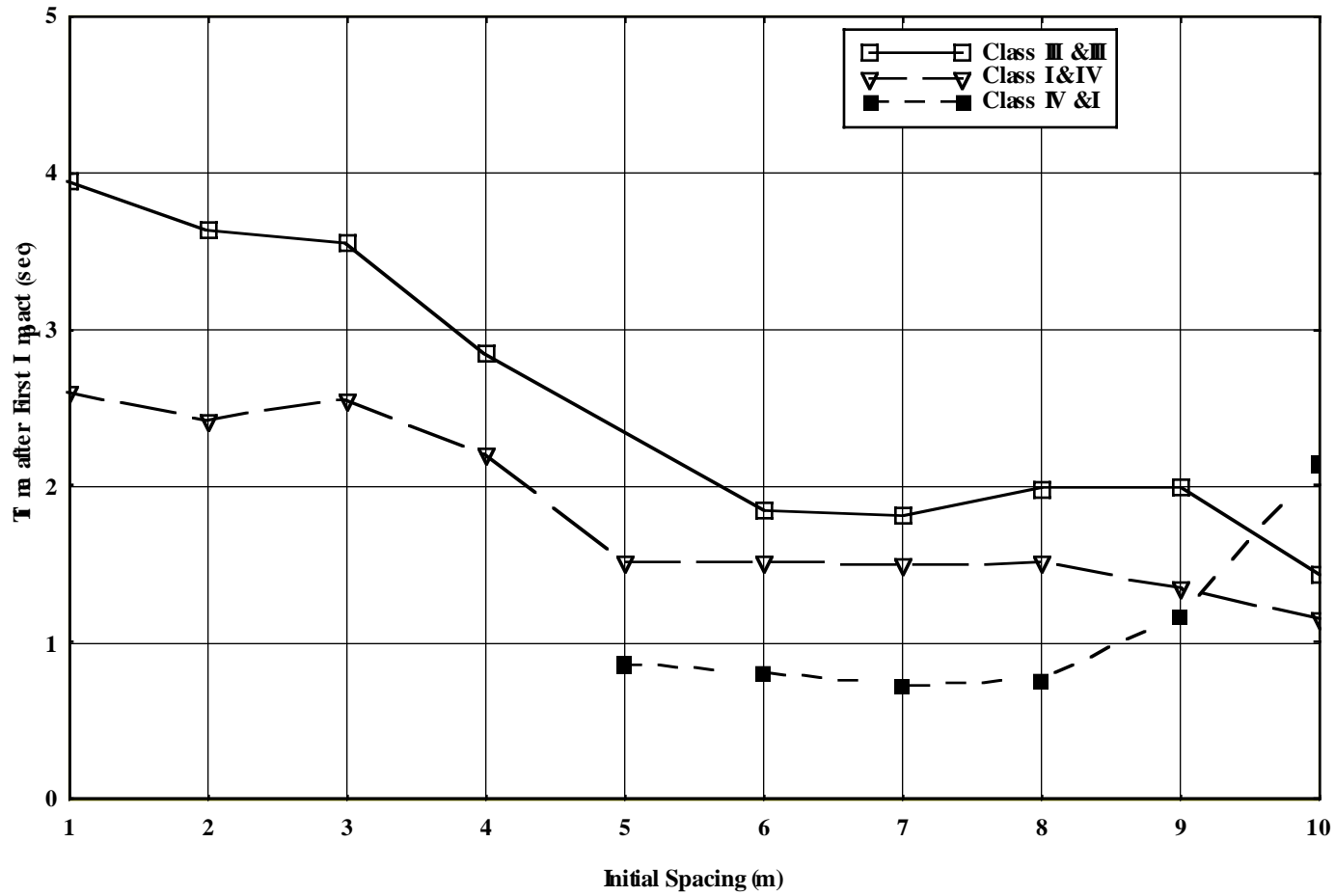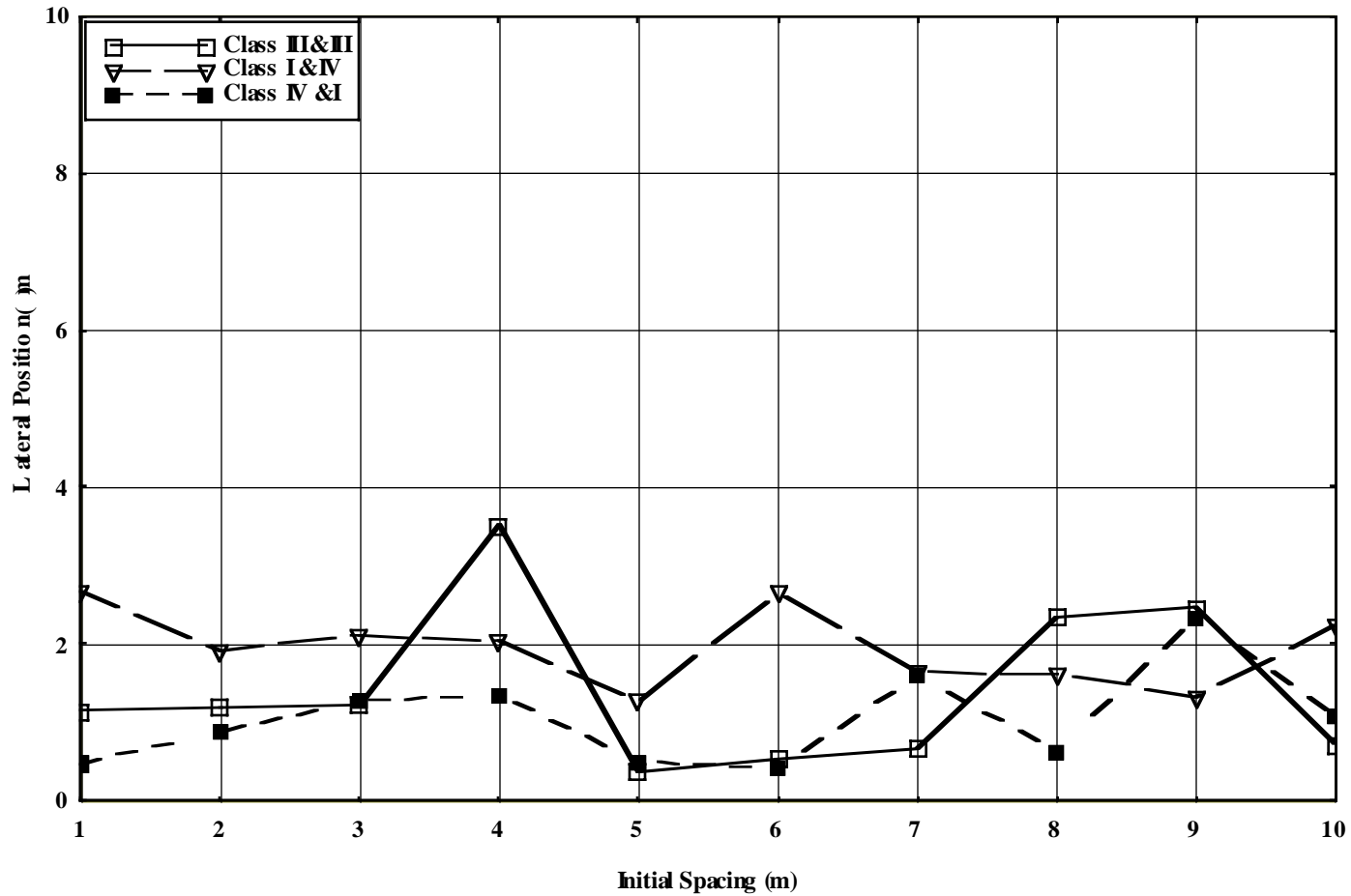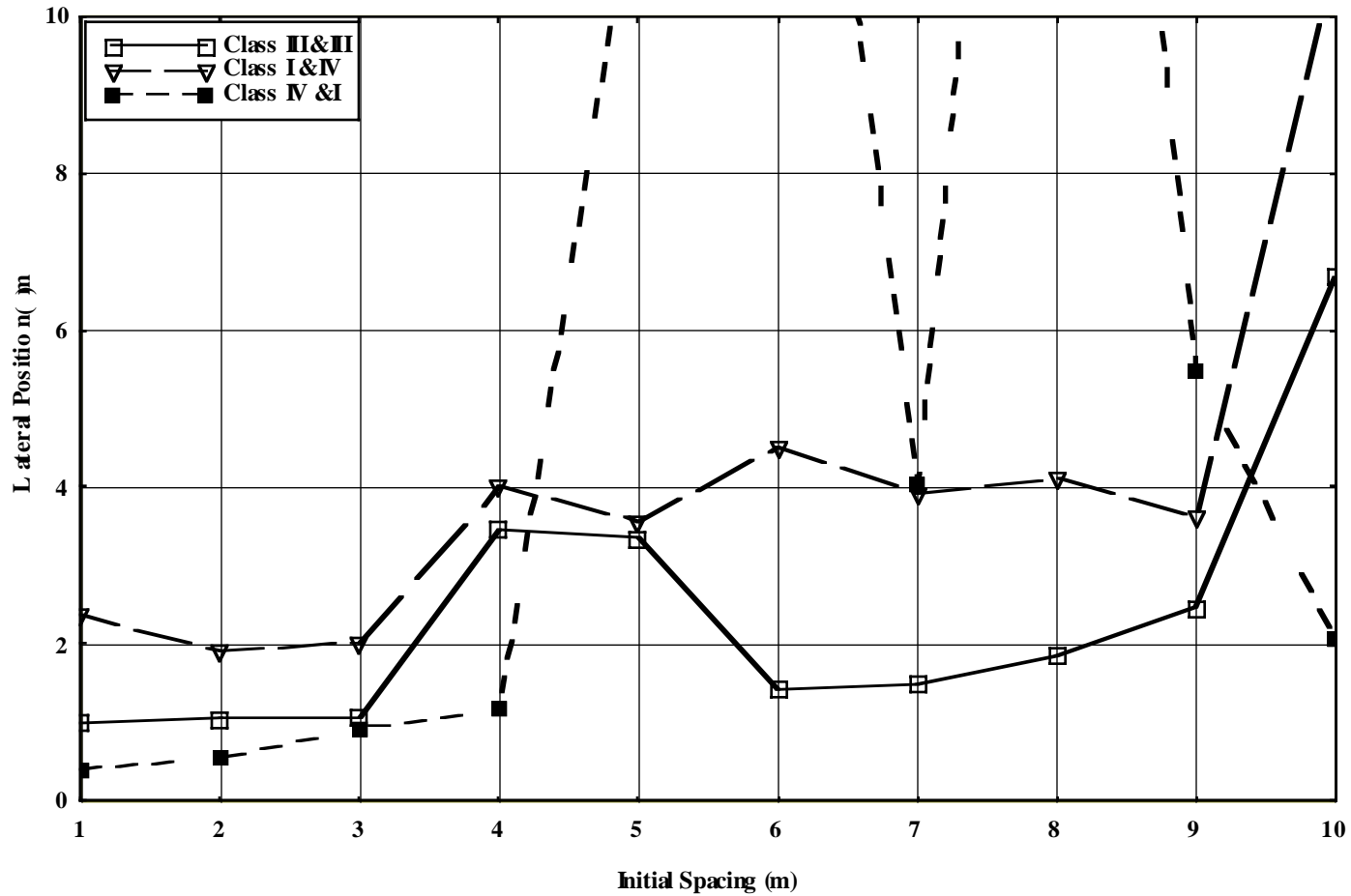
Figure 30. Maximum Abs(Lateral Position) of Following Vehicle with 105 kmph Initial Speed and 0.3 m Lateral Offset for Various Formations and Initial Spacing
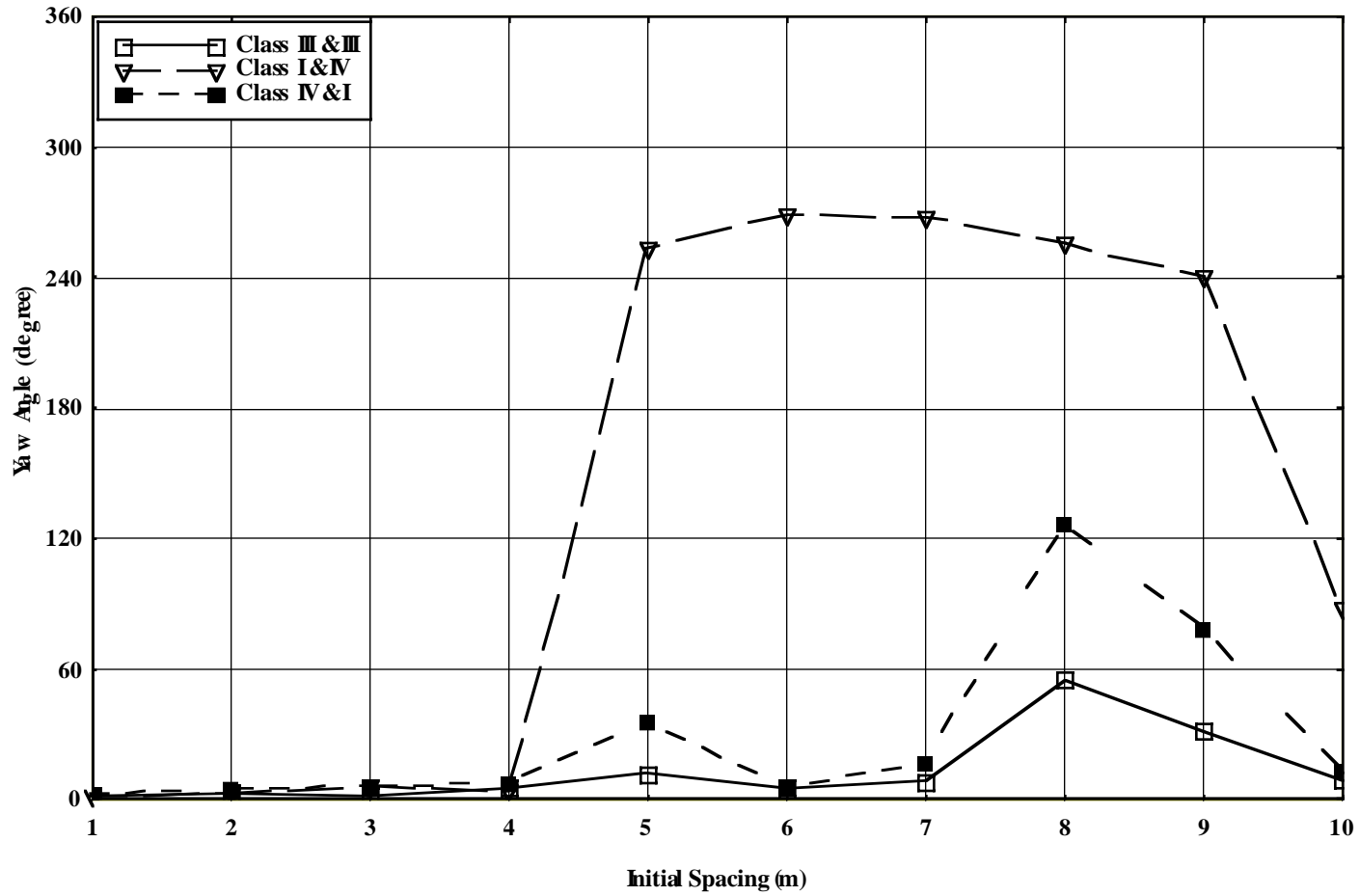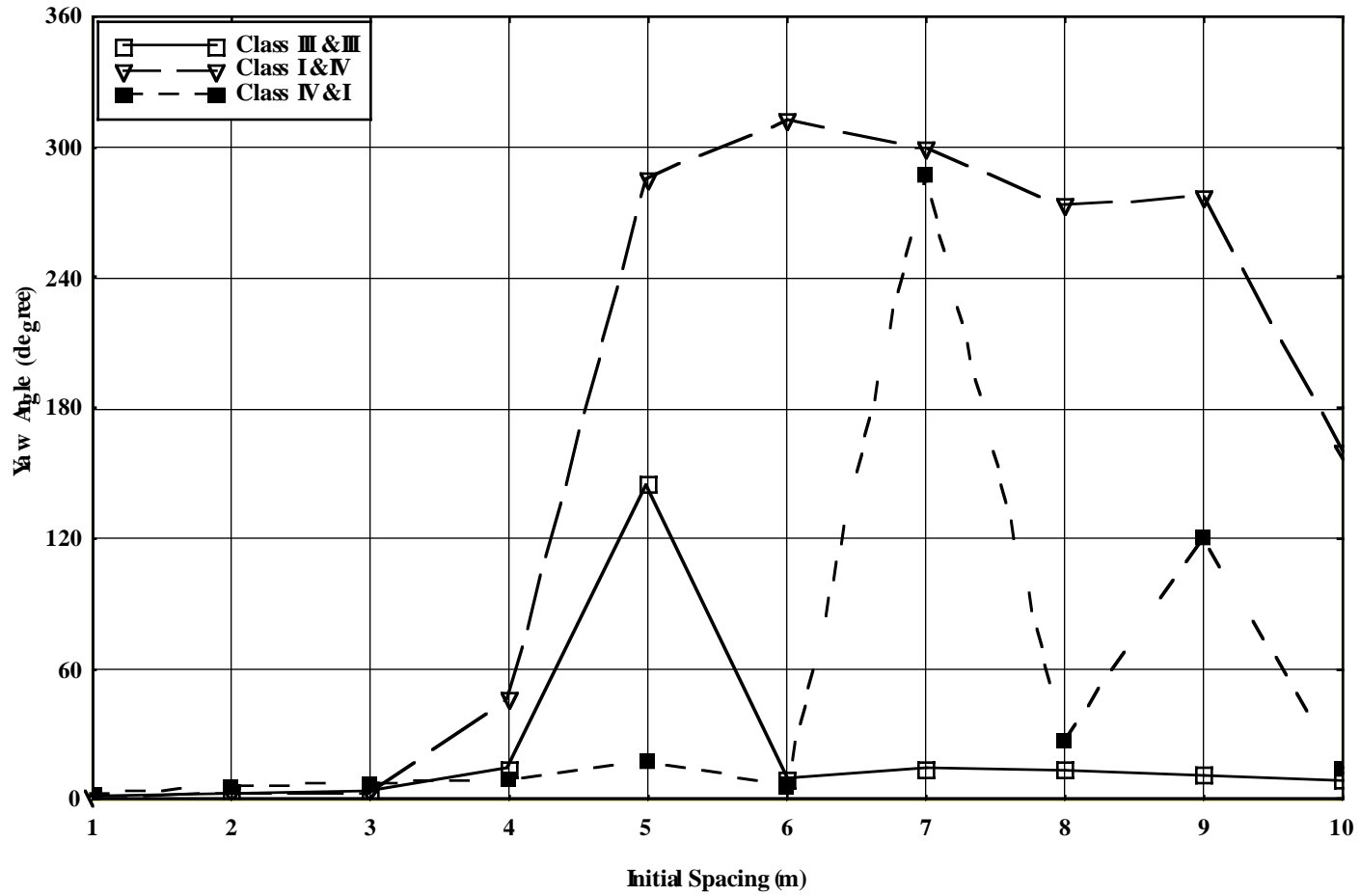
Figure 31. Maximum Abs(Yaw Angle) of Leading Vehicle with 105 kmph Initial Speed and 0.3 m Lateral Offset for Various Formations and Initial Spacing
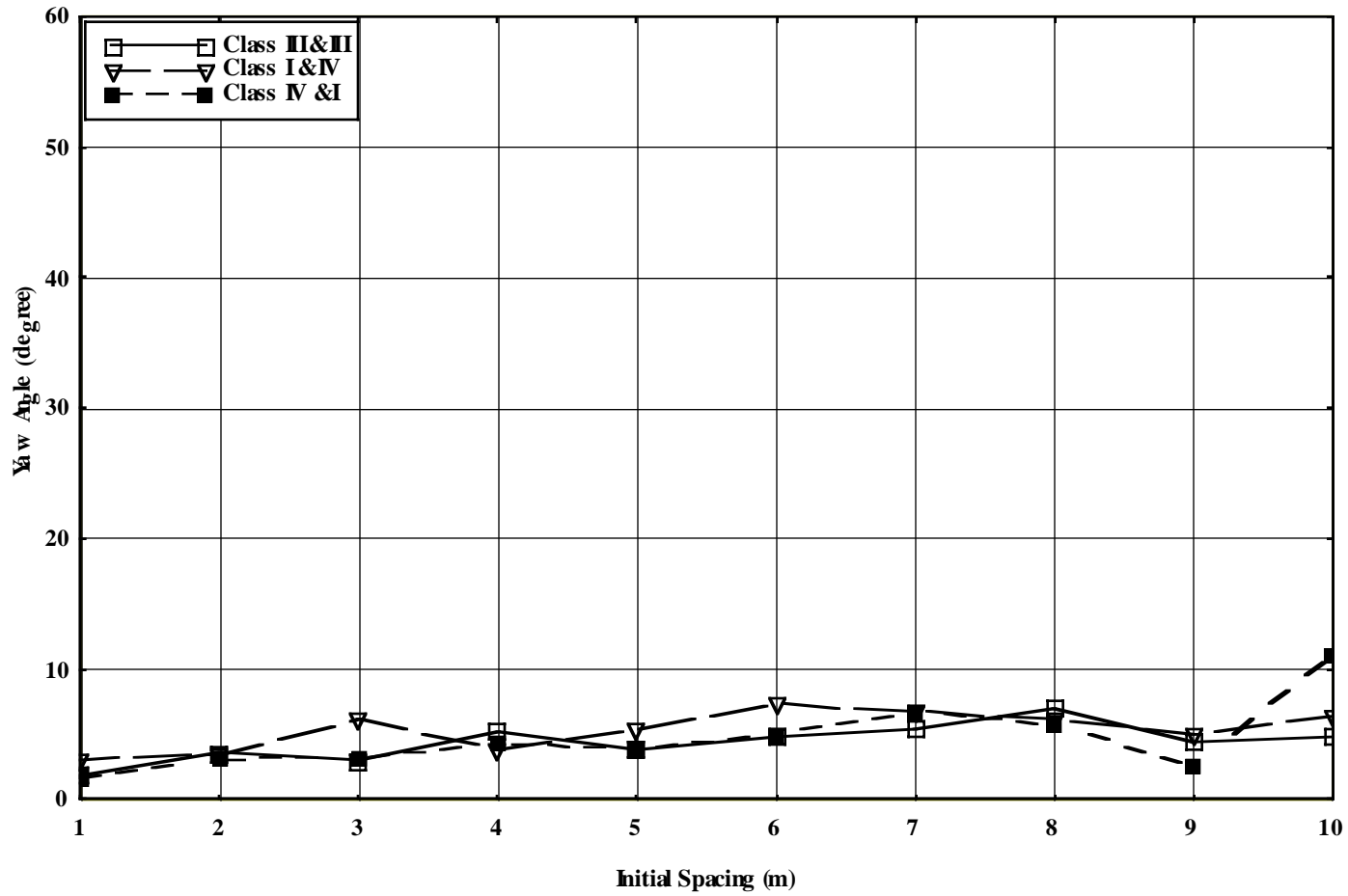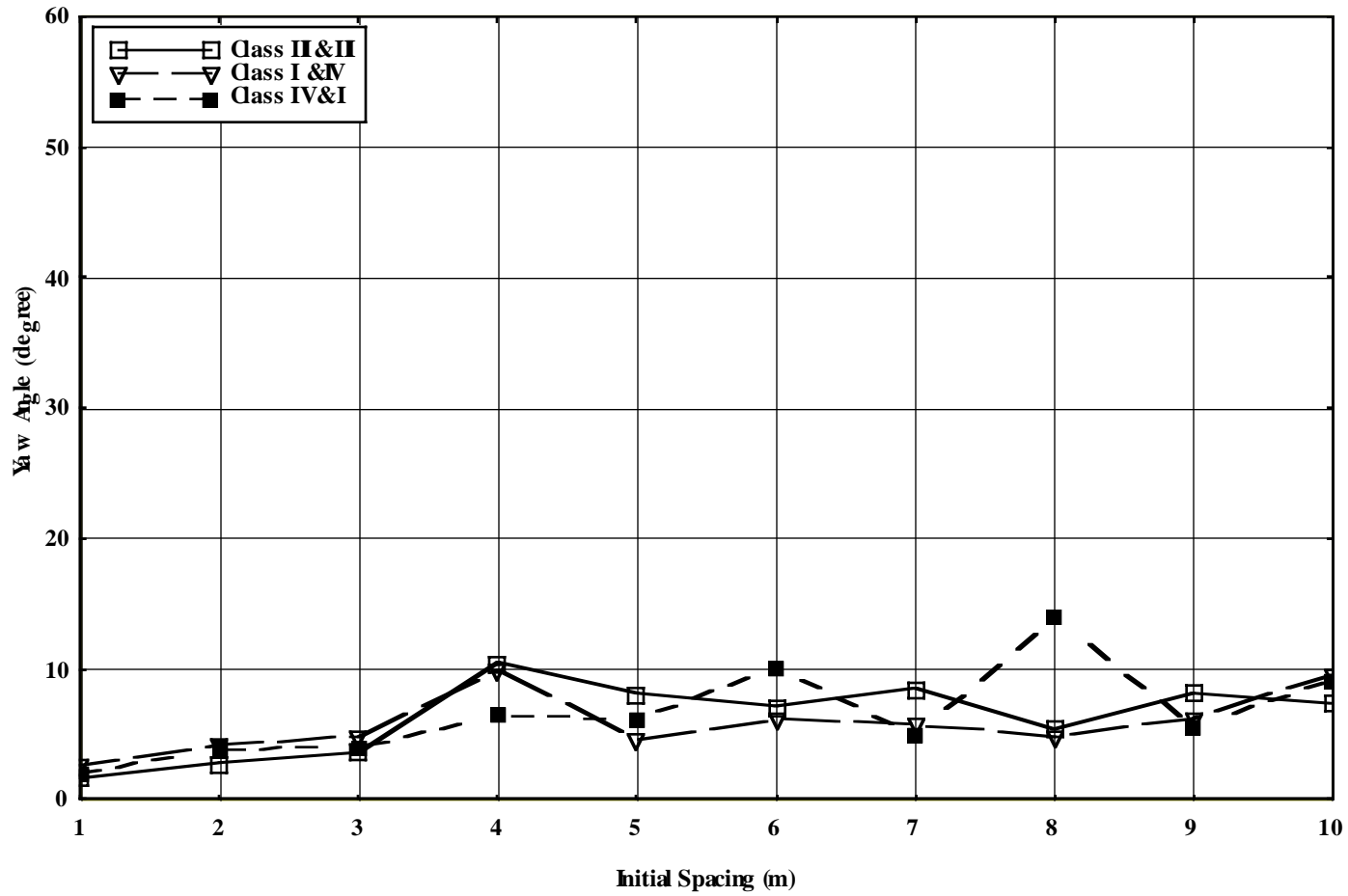
Figure 32. Maximum Abs(Yaw Angle) of Following Vehicle with 105 kmph Initial Speed and 0.3 m Lateral Offset for Various Formations and Initial Spacing
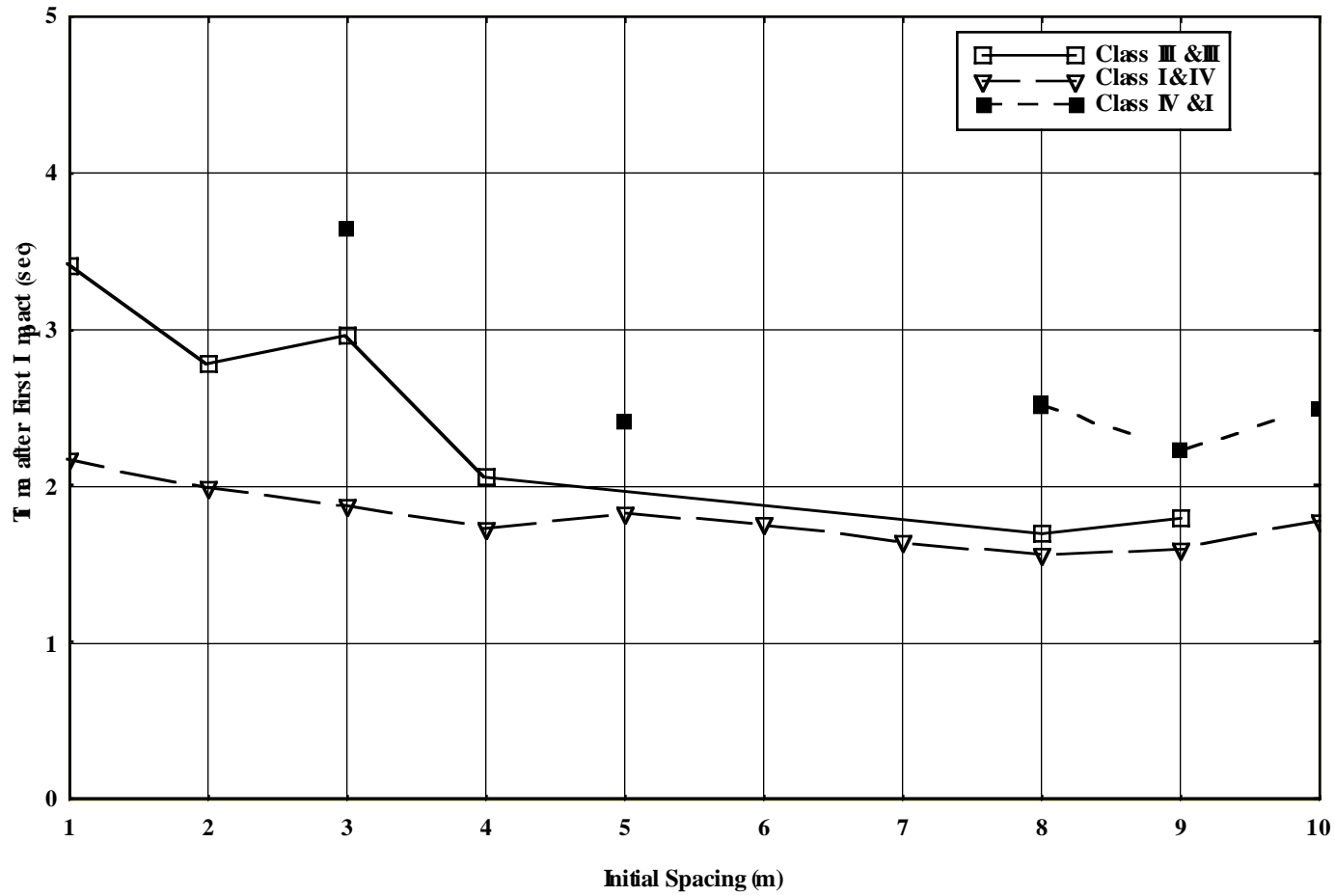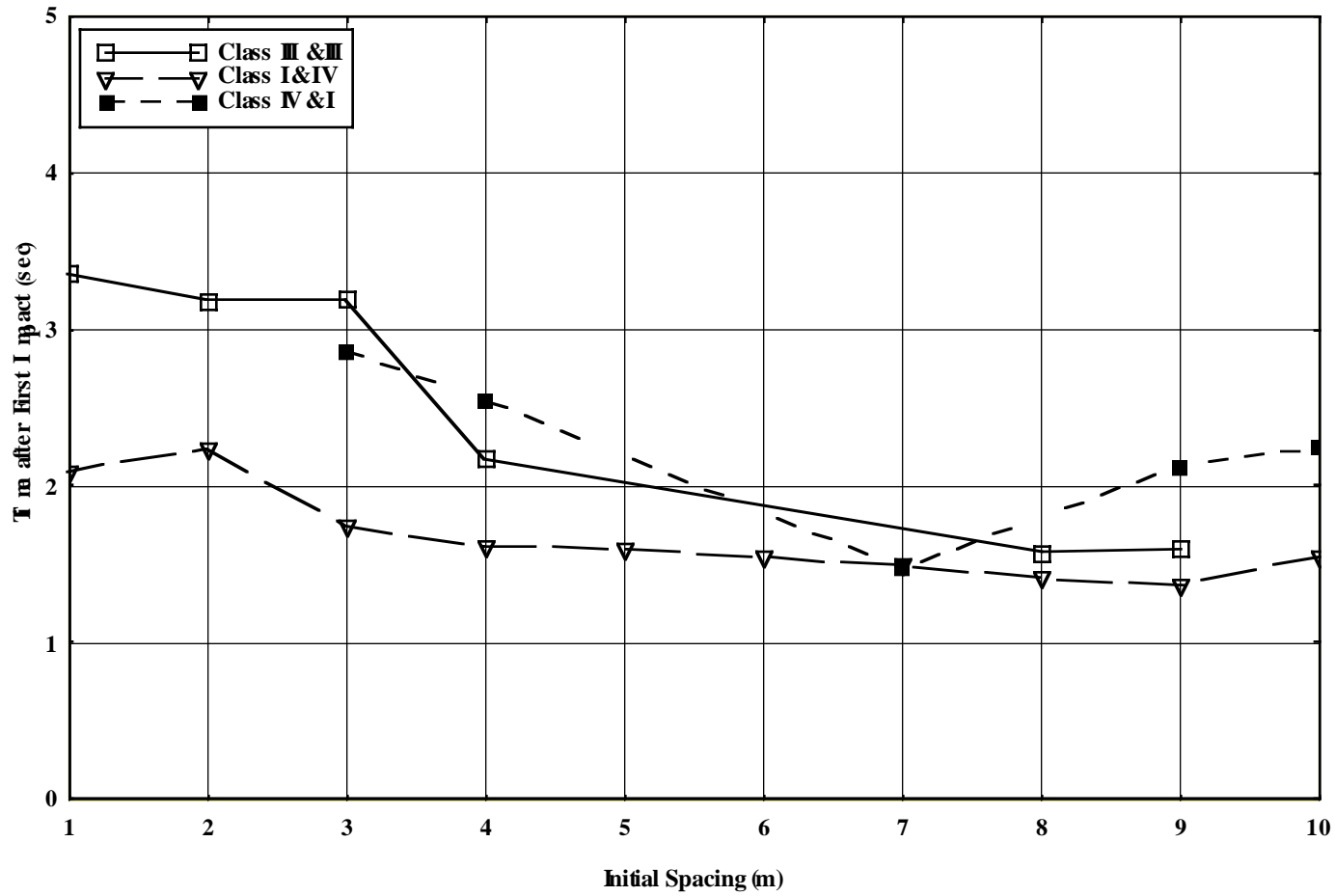
Figure 33. Lane Departure Time of Leading Vehicle with 105 kmph Initial Speed and 0.3 m Lateral Offset for Various Formations and Initial Spacing

Figure 34. Lane Departure Time of Following Vehicle with 105 kmph Initial Speed and 0.3 m Lateral Offset for Various Formations and Initial Spacing

Figure 35. Maximum Abs(Lateral Position) of Leading Vehicle with 153 kmph Initial Speed and 0.3 m Lateral Offset for Various Formations and Initial Spacing

Figure 36. Maximum Abs(Lateral Position) of Following Vehicle with 153 kmph Initial Speed and 0.3 m Lateral Offset for Various Formations and Initial Spacing

Figure 37. Maximum Abs(Yaw Angle) of Leading Vehicle with 153 kmph Initial Speed and 0.3 m Lateral Offset for Various Formations and Initial Spacing

Figure 38. Maximum Abs(Yaw Angle) of Following Vehicle with 153 kmph Initial Speed and 0.3 m Lateral Offset for Various Formations and Initial Spacing

Figure 39. Lane Departure Time of Leading Vehicle with 153 kmph Initial Speed and 0.3 m Lateral Offset for Various Formations and Initial Spacing
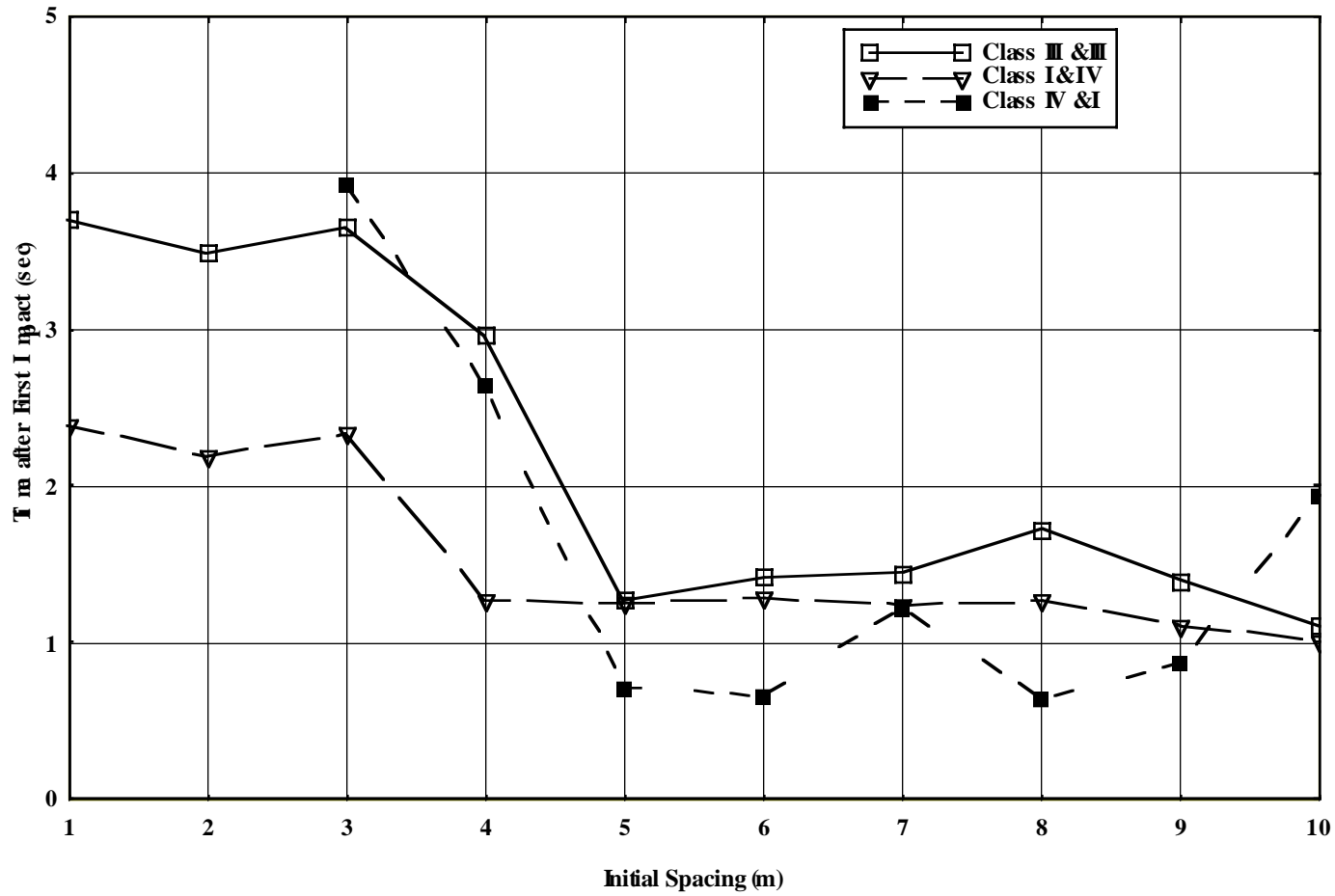
Figure 40. Lane Departure Time of Following Vehicle with 153 kmph Initial Speed and 0.3 m Lateral Offset for Various Formations and Initial Spacing
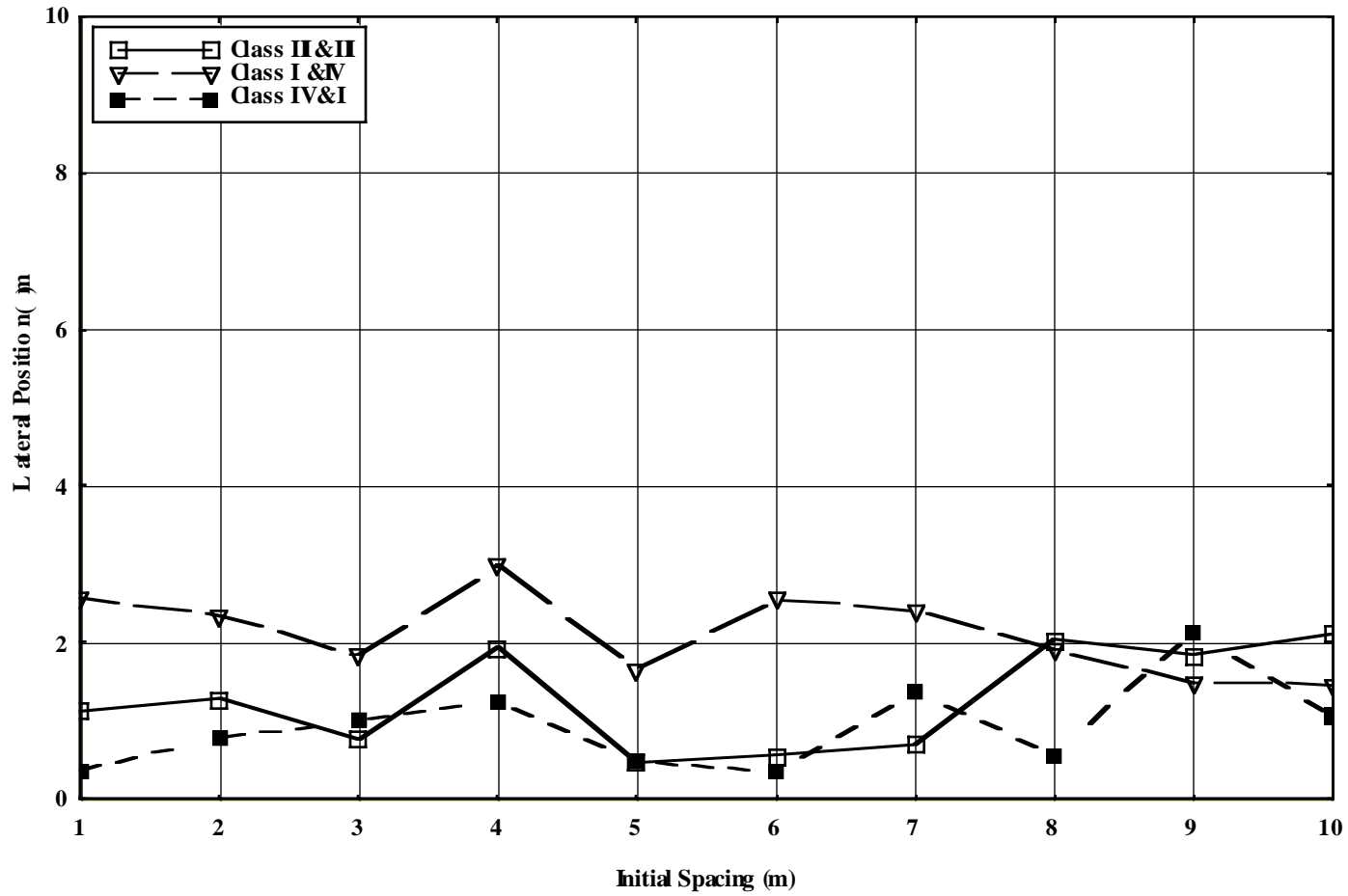
Figure 41. Maximum Abs(Lateral Position) of Leading Vehicle with 129 kmph Initial Speed and 0.3 m Lateral Offset for Various Formations and Initial Spacing
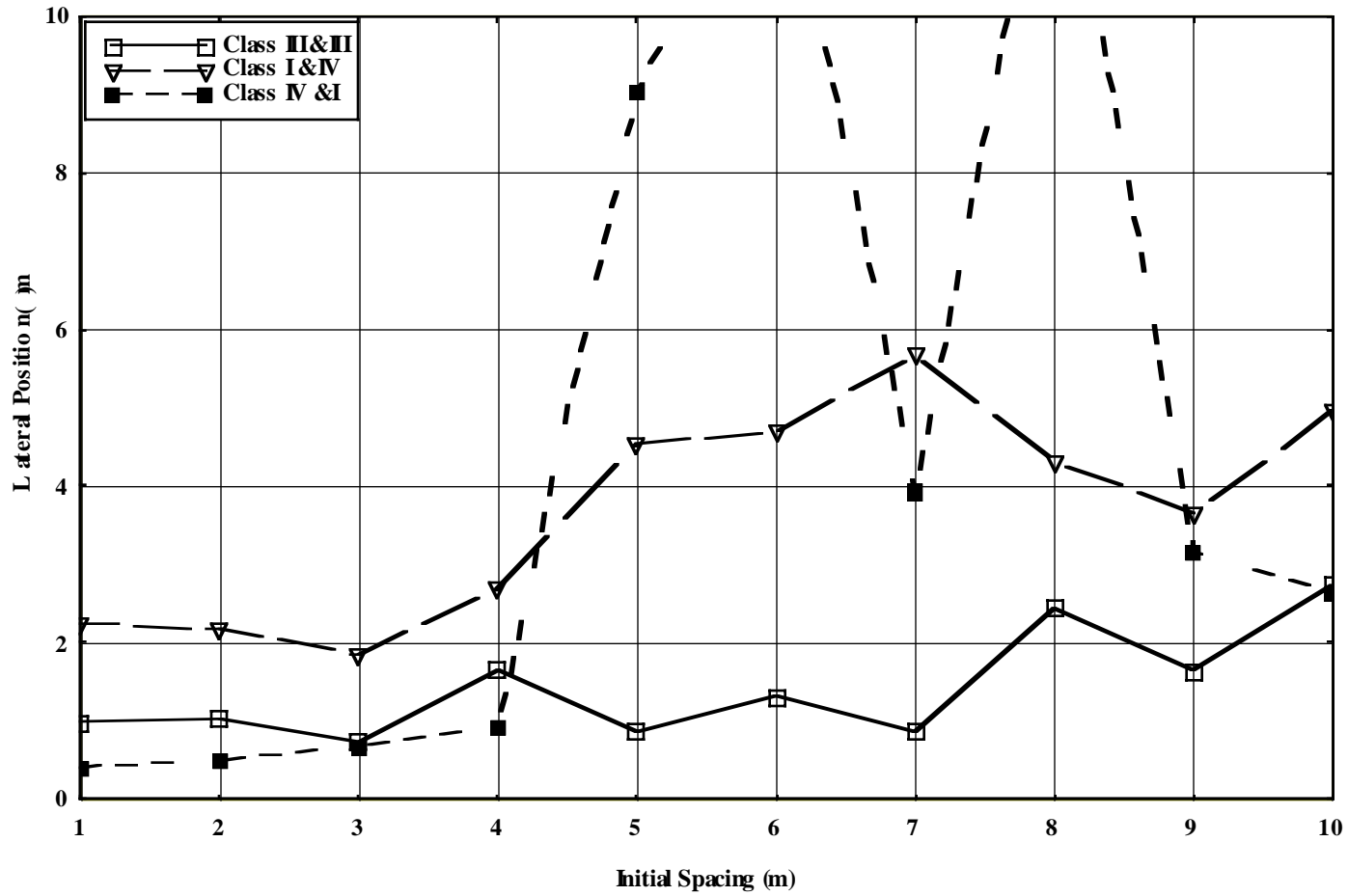
Figure 42. Maximum Abs(Lateral Position) of Following Vehicle with 129 kmph Initial Speed and 0.3 m Lateral Offset for Various Formations and Initial Spacing
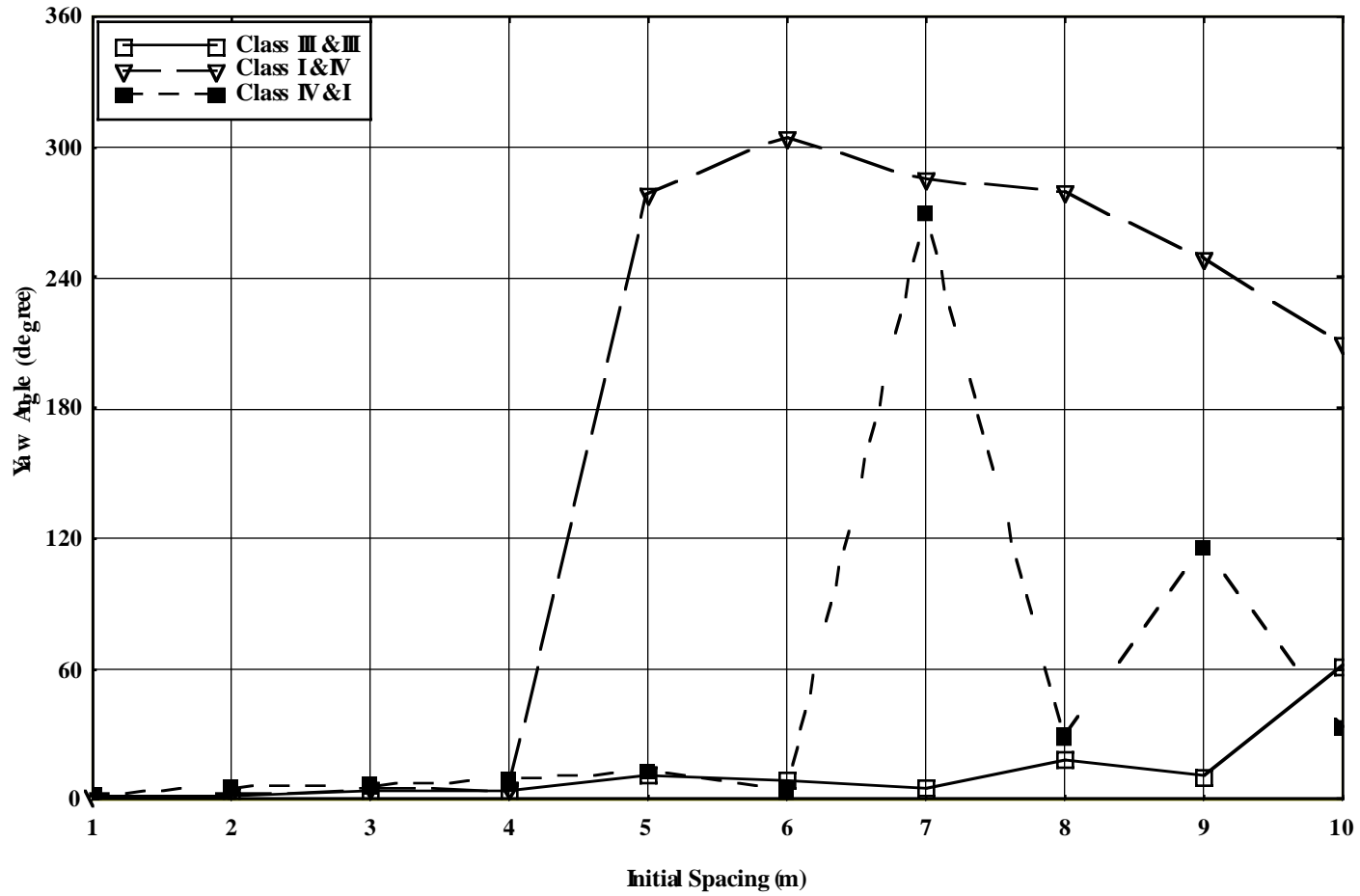
Figure 43. Maximum Abs(Yaw Angle) of Leading Vehicle with 129 kmph Initial Speed and 0.3 m Lateral Offset for Various Formations and Initial Spacing
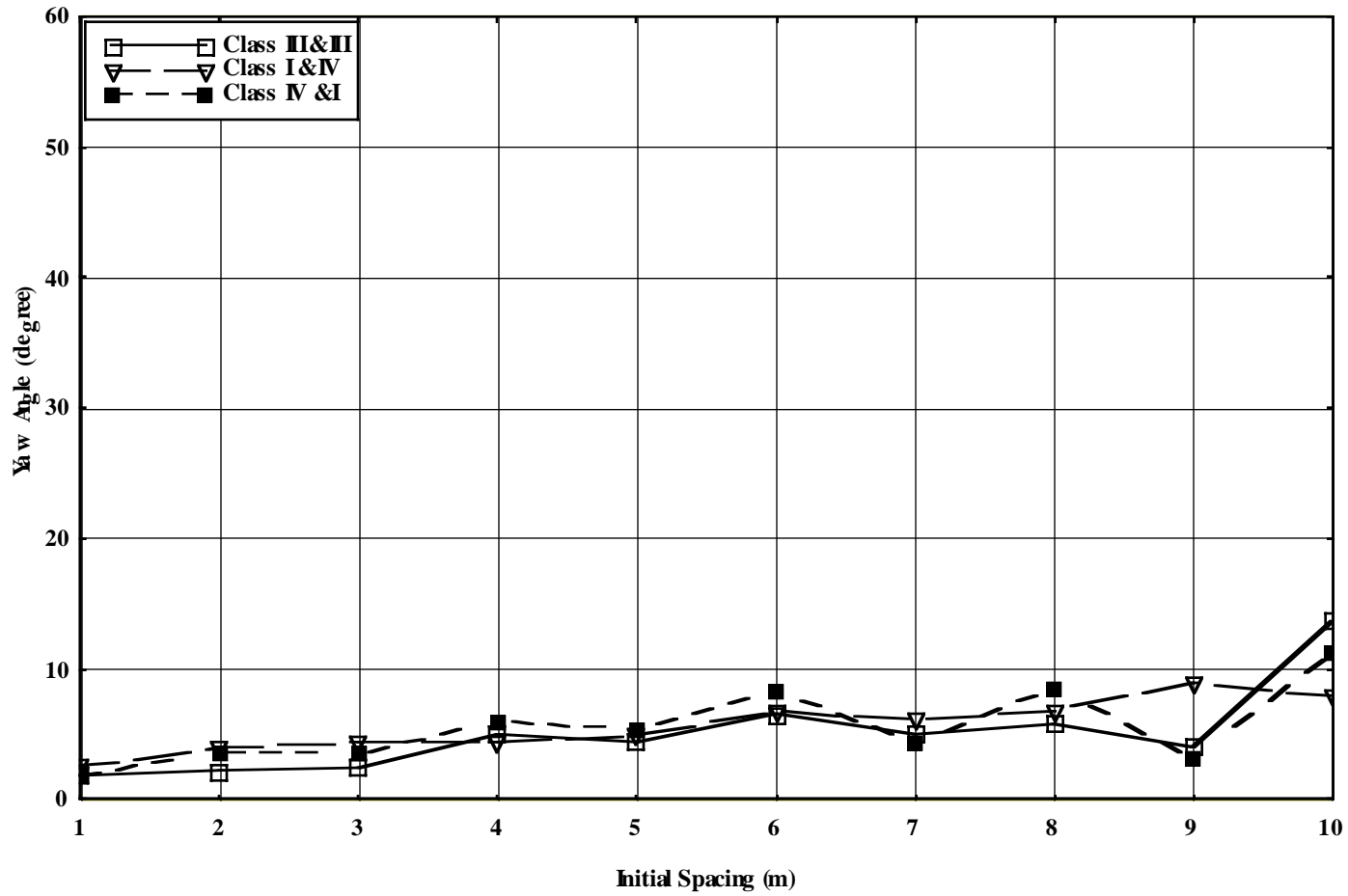
Figure 44. Maximum Abs(Yaw Angle) of Following Vehicle with 129 kmph Initial Speed and 0.3 m Lateral Offset for Various Formations and Initial Spacing
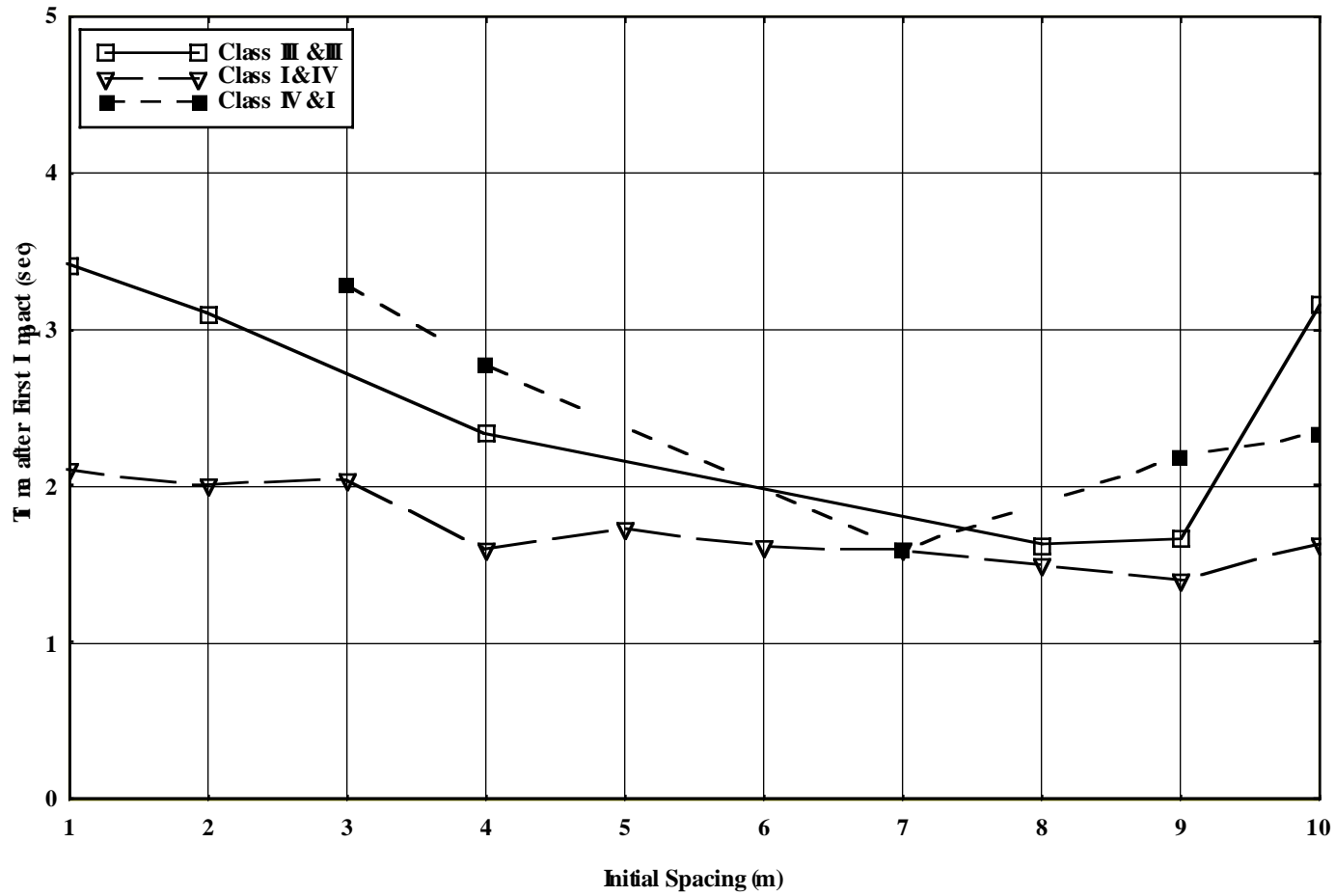
Figure 45. Lane Departure Time of Leading Vehicle with 129 kmph Initial Speed and 0.3 m Lateral Offset for Various Formations and Initial Spacing
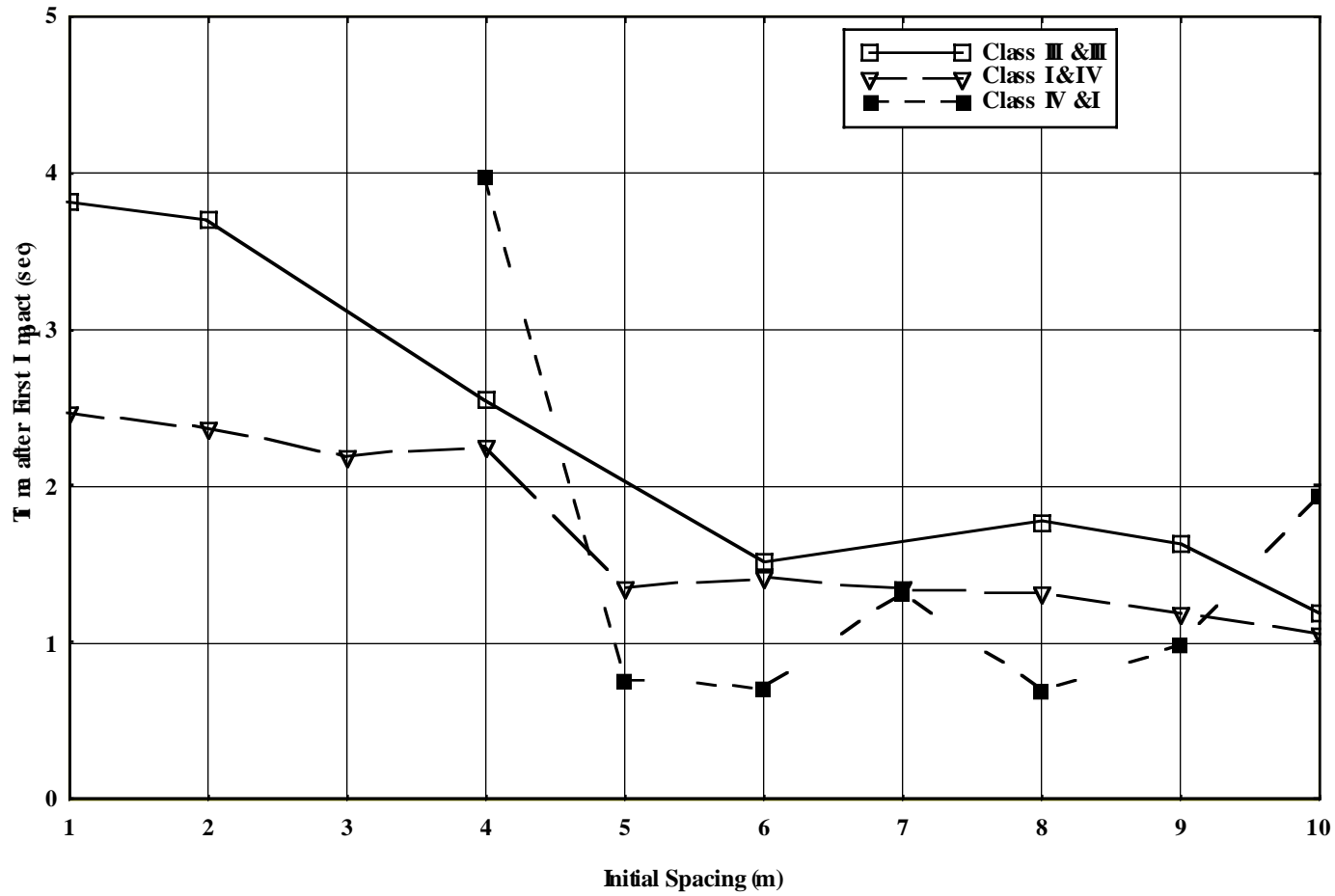
Figure 46. Lane Departure Time of Following Vehicle with 129 kmph Initial Speed and 0.3 m Lateral Offset for Various Formations and Initial Spacing